Synthesis and Structural Characterization of Bimetallic μ-Malonyl Complexes

Joseph M. O'Connor,*[1a] Roger Uhrhammer,[1a] Arnold L. Rheingold,*[1b] Donna L. Staley,[1b] and Raj K. Chadha[1c]

Contribution from the Departments of Chemistry, University of California at San Diego, La Jolla, California 92093, and University of Delaware, Newark, Delaware 19716.
Received April 4, 1990

Abstract: Reaction of rhenaenolate $[(\eta^5\text{-}C_5Me_5)(NO)(PPh_3)Re(COCH_2)]^-Li^+$ (**8**), generated from $(\eta^5\text{-}C_5Me_5)(NO)(PPh_3)Re(COCH_3)$ (**9**) and *n*-BuLi, with $(CO)_5M(OSO_2CF_3)$ [M = Re, Mn] leads to good yields of the μ-η^1,η^2-malonyl complexes $(\eta^5\text{-}C_5Me_5)(NO)(PPh_3)Re[\mu\text{-}(COCH_2CO)\text{-}C^1{:}C^3,O^1]M(CO)_4$ (M = Re (**10-Re**), Mn (**10-Mn**)). In THF solution **10-Re** exists in equilibrium with its enol tautomer $(\eta^5\text{-}C_5Me_5)(NO)(PPh_3)Re[\mu\text{-}(COCH{=}C(OH))\text{-}C^1,O^3{:}C^3]Re(CO)_4$ (**14-Re**) ($K_{eq}^{23°C}$ = [**14-Re**]/[**10-Re**] = 0.66). In contrast, the enol form of **10-Mn** is not observed in THF solvent. Reaction of **8** and $(CO)_5ReBr$ generates an isolable anionic malonyl complex $\{(\eta^5\text{-}C_5Me_5)(NO)(PPh_3)Re[\mu\text{-}(COCH_2CO)\text{-}C^1{:}C^3]Re(CO)_4(Br)\}^-Li^+$ (**17**), in which the malonyl ligand chelates a lithium cation. Complex **17** does not enolize to an observable extent (by ^1H NMR spectroscopy) in THF solvent. The lithium ion in **17** is readily exchanged with a magnesium bromide cation to give $\{(\eta^5\text{-}C_5Me_5)(NO)(PPh_3)Re[\mu\text{-}(COCH_2CO)\text{-}C^1{:}C^3]Re(CO)_4(Br)\}^-MgBr^+$ (**18**). Treatment of **17** with 12-crown-4 results in loss of the bromide ligand and conversion to **10-Re**. Reaction of **8** with $[Re(CO)_5(PMe_3)]^+OSO_2CF_3^-$ gives the neutral, lithium ion chelated complex $\{(\eta^5\text{-}C_5Me_5)(NO)(PPh_3)Re[\mu\text{-}(COCH_2CO)\text{-}C^1{:}C^3]Re(CO)_4(PMe_3)\}\cdot Li^+OSO_2CF_3^-$ (**19**). The reaction of **8** and $Re(CO)_5(OSO_2CF_3)$ proceeds via an intermediate that is observable by NMR spectroscopy at low temperature. This intermediate was trapped with PMe_3 at −76 °C to give **19**. The IR ν(C=O) stretching frequencies in the malonyl ligand of **10-Re**, **17**, and **19** were assigned with the aid of isotopic labeling at the carbonyl carbons. Complexes **17** and **19** exhibit differential $^2J_{CH}$ coupling between the carbonyl carbons and the methylene hydrogens of the malonyl ligand. This differential coupling is a potentially useful probe of malonyl and acyl ligand conformation.

Introduction

The structure, properties, and reactivity of "β-oxoacyl" or "malonyl" complexes, I and II, remain virtually unexplored due to the remarkably elusive nature of this compound class. As with typical metal acyls, III, interest in β-oxoacyls stems from the potential role of these compounds as intermediates in organic synthesis,[2] as well as the implications that their properties and reactivity hold for carbon monoxide homologation chemistry.[3] Formally, the malonyl ligand in II may be derived via either a double carbonylation of a μ-methylene species[3] or coupling of a ketene and carbon monoxide molecule.[4]

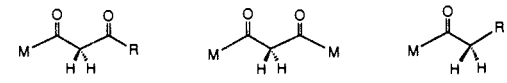

I II III

β-Oxoacyl complexes are expected to afford a number of significant structural and reactivity differences from those observed for simple metal acyls of type III. Clearly, the presence of the additional carbonyl function will lead to increased acidity at the methylene hydrogens. This in turn leads to the possibility of keto–enol tautomerization—a phenomenon not previously observed in transition-metal acyl complexes.[5] Enhanced acidity will also allow for direct generation of quaternary carbon centers via sequential deprotonation–alkylation chemistry;[6] once again this is in contrast to simple metal acyls for which quaternary carbons are not generally accessible by such a route.[7] The stability and reactivity of the β-oxoacyl ligand may also be modified by introduction of an additional metal via 1,3-dicarbonyl chelation chemistry.[8] Finally, initial indications are that β-oxoacyl complexes contain a more labile carbon–carbon bond compared to that in known metal acyl complexes.[9]

(1) (a) University of California, San Diego. (b) University of Delaware. (c) University of California, San Diego X-ray Crystallography Facility.

(2) (a) Rusik, C. A.; Collins, M. A.; Gamble, A. S.; Tonker, T. L.; Templeton, J. L. *J. Am. Chem. Soc.* **1989**, *111*, 2550. (b) Constable, A. G.; Gladysz, J. A. *J. Organomet. Chem.* **1980**, *202*, C21. Kiel, W. A.; Lin, G.-Y.; Bodner, G. S.; Gladysz, J. A. *J. Am. Chem. Soc.* **1983**, *105*, 4958. Crocco, G. L.; Gladysz, J. A. *J. Am. Chem. Soc.* **1985**, *107*, 4103. O'Connor, E. J.; Kobayashi, M.; Floss, H. G.; Gladysz, J. A. *J. Am. Chem. Soc.* **1987**, *109*, 4837. Bodner, G. S.; Smith, D. E.; Hatton, W. G.; Heah, P. C.; Georgiou, S.; Rheingold, A. L.; Geib, S. J.; Hutchinson, J. P.; Gladysz, J. A. *J. Am. Chem. Soc.* **1987**, *109*, 7688. Buhro, W. E.; Zwick, B. D.; Georgiou, S.; Hutchinson, J. P.; Gladysz, J. A. *J. Am. Chem. Soc.* **1988**, *110*, 2427. (c) Liebeskind, L. S.; Welker, M. E. *Organometallics* **1983**, *2*, 194. Liebeskind, L. S.; Welker, M. E.; Goedken, V. *J. Am. Chem. Soc.* **1984**, *106*, 441. Liebeskind, L. S.; Fengl, R. W.; Welker, M. E. *Tetrahedron Lett.* **1985**, *26*, 3075. Liebeskind, L. S.; Welker, M. E.; Fengl, R. W. *J. Am. Chem. Soc.* **1986**, *108*, 6328. (d) Baird, G. J.; Davies, S. G. *J. Organomet. Chem.* **1983**, *248*, C1. Ambler, P. W.; Davies, S. G. *Tetrahedron Lett.* **1985**, *26*, 2129. Baird, G. J.; Davies, S. G.; Maberly, T. R. *Organometallics* **1984**, *3*, 1964. Ayscough, A. P.; Davies, S. G. *J. Chem. Soc., Chem. Commun.* **1986**, 1648. Davies, S. G.; Dordor-Hedgecock, I. M.; Warner, P.; Jones, R. H.; Prout, K. *J. Organomet. Chem.* **1985**, *285*, 213. Davies, S. G.; Dordor-Hedgecock, I. M.; Warner, P. *Tetrahedron Lett.* **1985**, *26*, 2125. Brown, S. L.; Davies, S. G.; Warner, P.; Jones, R. H.; Prout, K. *J. Chem. Soc., Chem. Commun.* **1985**, 1446. Davies, S. G.; Walker, J. C. *J. Chem. Soc., Chem. Commun.* **1986**, 609. Brown, S. L.; Davies, S. G.; Foster, D. F.; Seeman, J. I.; Warner, P. *Tetrahedron Lett.* **1986**, *27*, 623. Seeman, J. I.; Davies, S. G. *J. Am. Chem. Soc.* **1985**, *107*, 6522. Davies, S. G. *Pure Appl. Chem.* **1988**, *60*, 13 and references therein. (e) Theopold, K. H.; Becker, P. N.; Bergman, R. G. *J. Am. Chem. Soc.* **1982**, *104*, 5250. Doney, J. J.; Bergman, R. G.; Heathcock, C. H. *J. Am. Chem. Soc.* **1985**, *107*, 3724. Burkhardt, E. R.; Doney, J. J.; Stack, J. G.; Heathcock, C. H.; Bergman, R. G. *J. Mol. Catal.* **1987**, *41*, 41. Burkhardt, E. R.; Doney, J. J.; Slough, G. A.; Stack, J. M.; Heathcock, C. H.; Bergman, R. G. *Pure Appl. Chem.* **1988**, *60*, 1 and references therein. (f) Brown-Wensley, K. A.; Buchwald, S. L.; Canizzo, L.; Clawson, L.; Ho, S.; Meinhardt, D.; Stille, J. R.; Straus, D.; Grubbs, R. H. *Pure Appl. Chem.* **1983**, *55*, 1733. (g) Brinkman, K.; Helquist, P. *Tetrahedron Lett.* **1985**, *26*, 2845.

(3) (a) Denise, B.; Navarre, D.; Rudler, H.; Daran, J. C. *J. Organomet. Chem.* **1989**, *375*, 273. (b) Roper, M.; Strutz, H.; Keim, W. *J. Organomet. Chem.* **1981**, *219*, C5. (c) Navarre, D.; Rose-Munch, F.; Rudler, H. *J. Organomet. Chem.* **1985**, *284*, C15. (d) Navarre, D.; Rudler, H.; Daran, J. C. *J. Organomet. Chem.* **1986**, *314*, C34.

(4) Ube Industries, Ltd., Eur. Pat. Appl. 6611 (Cl. CO7C69138, 1980; *Chem. Abstr.* **1980**, *93*, 45987.

(5) O'Connor, J. M.; Uhrhammer, R. *J. Am. Chem. Soc.* **1988**, *110*, 4448.

(6) O'Connor, J. M.; Uhrhammer, R.; Rheingold, A. L. *Organometallics* **1988**, *7*, 2422.

(7) (a) Davies, S. G.; Walker, J. C. *J. Chem. Soc., Chem. Commun.* **1986**, 495. (b) Templeton has demonstrated that the α-carbon of η^2-acyls may be converted to a quaternary center via deprotonation/alkylation: Rusik, C. A; Tonker, T. L.; Templeton, J. L. *J. Am. Chem. Soc.* **1986**, *108*, 1652.

(8) O'Connor, J. M.; Uhrhammer, R.; Rheingold, A. L.; Staley, D. L. *J. Am. Chem. Soc.* **1989**, *111*, 7633.

(9) Davies, S. G.; Watts, O.; Aktogu, N.; Felkin, H. *J. Organomet. Chem.* **1983**, *243*, C51.

0002-7863/90/1512-7585$02.50/0

Scheme I

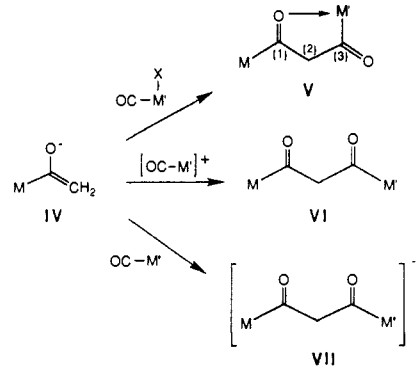

To date only two examples of mononuclear β-oxoacyl complexes have been isolated: $(CO)_2(NO)(PPh_3)Fe[C(=O)CH_2CO_2Et]$ (**1**), prepared from triphenylphosphine and $(CO)_3(NO)Fe(CH_2CO_2Et)$;[10] and $(PPh_3)_2(Cl)_2Ir[C(=O)CH_2COOEt]$ (**2**), formed upon oxidative addition of ethyl malonyl chloride to $(PPh_3)_2(N_2)Ir(Cl)$.[11] Palyi and co-workers found that the 2-oxoalkyl cobalt complex $(CO)_4Co(CH_2CO_2Et)$ undergoes reaction with triphenylphosphine to give an unstable cobalt oxoacyl, $(CO)_3(PPh_3)Co[C(=O)CH_2CO_2Et]$ (**3**), which undergoes spontaneous decarbonylation at 20 °C to give $(CO)_3(PPh_3)Co(CH_2CO_2Et)$.[12]

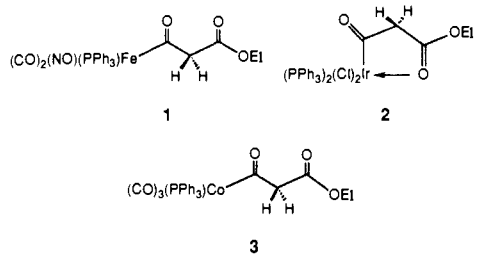

In contrast to the preparation of **1**, Cutler found that $(\eta^5\text{-}C_5H_5)(CO)_2Fe(CH_2CO_2Me)$ is inert toward carbonylation under a variety of conditions.[13] Consistent with Cutler's observation is a report by Akita that the bimetallic μ-ketene complex $[(\eta^5\text{-}C_5H_5)(CO)_2Fe]_2[\mu\text{-}(CH_2CO)\text{-}C^1{:}C^2]$ (**4**) is inert toward carbonylation to the μ-malonyl complex **5**.[14] Indeed, prior to our work in this area, the only example of a stable bimetallic μ-malonyl complex was for the difluoro derivative $[(CO)_5Mn]_2[\mu\text{-}(COCF_2CO)\text{-}C^1{:}C^2]$, prepared by reaction of $[(CO)_5Mn]^-Na^+$ and dichloro difluoromalonate.[15]

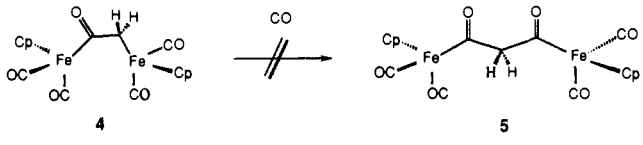

Other, potentially straightforward routes toward mononuclear β-oxoacyl complexes have met with frustration. Cutler observed an 85% yield of the iron hydride $(\eta^5\text{-}C_5H_5)(CO)_2Fe(H)$ upon reaction of $(\eta^5\text{-}C_5H_5)(CO)_2Fe^-K^+$ and ethyl malonyl chloride,[16] and Davies employed the reaction of the metallaenolate $(\eta^5\text{-}C_5H_5)(CO)(PPh_3)Fe(COCH_2)]^-Li^+$ (**6**) and an acyl halide in an attempt to generate the β-oxoacyl species **7**.[9] Although **7** was not observed, the formation of the iron carbonyl cation $(\eta^5\text{-}C_5H_5)(CO)_2(PPh_3)Fe^+$ and products derived from $RCOCH_2^-$ was indicative of initial formation of **7** followed by spontaneous carbon–carbon bond fragmentation.

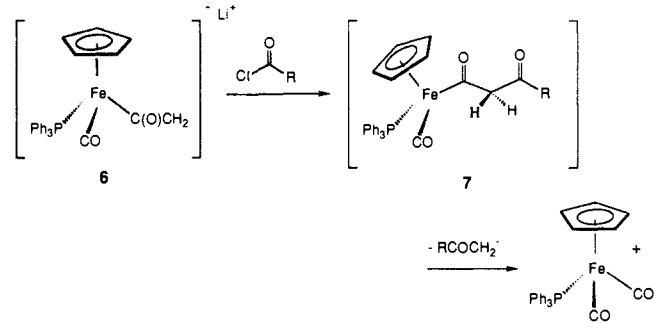

Our approach toward bimetallic μ-malonyl complexes involves the use of metallaenolates, IV, as intermediates in reactions with transition-metal carbonyl electrophiles (Scheme I).[17a] Thus reaction of a transition-metal enolate with a neutral metal carbonyl that contains a leaving group (X) is expected to generate a bimetallic μ-malonyl-$(C^1{:}C^3,O^1)$ complex, V, in which the malonyl oxygen is coordinated to one of the transition metals.[17b] Alternatively, reaction of a metallaenolate with a cationic carbonyl complex would generate a neutral μ-malonyl-$(C^1{:}C^3)$, VI; and reaction with a neutral metal carbonyl complex would lead to an anionic μ-malonyl-$(C^1{:}C^3)$, VII.

In this paper we report full details on the conversion of metallaenolates and metal carbonyl electrophiles to bimetallic μ-malonyl complexes—the first successful synthetic approach toward the preparation of the parent μ-malonyl complexes. By variation of the electrophile, three subclasses of μ-malonyl complexes were prepared: μ-malonyl-$(C^1{:}C^3,O^1)$, as well as neutral and anionic μ-malonyl-$(C^1{:}C^3)$ complexes. The mechanism of formation has been clarified by low-temperature NMR spectroscopy and trapping experiments. The structure and bonding for each type of malonyl complex were determined by NMR spectroscopy and X-ray crystallography. Geminal carbon–hydrogen couplings between the methylene hydrogens and the carbonyl carbons of the malonyl ligand show promise as a diagnostic tool for malonyl and acyl ligand conformation. In the case of the neutral μ-malonyl-$(C^1{:}C^3)$, and anionic μ-malonyl-$(C^1{:}C^3)$ complexes, a lithium ion is chelated by the malonyl ligand. The neutral μ-malonyl-$(C^1{:}C^3)$ structure represents the only structurally characterized example of alkali metal chelation by a neutral malonyl compound. Portions of this work have appeared in preliminary form.[5,6,8,17a]

Results

1. Synthesis and Spectroscopic Characterization of Bimetallic μ-Malonyl Complexes: $(\eta^5\text{-}C_5Me_5)(NO)(PPh_3)Re[\mu\text{-}(COCH_2CO)\text{-}C^1{:}C^3,O^1]M(CO)_4$ (M = Re (10-Re), Mn (10-Mn)). Metallaenolates have previously been employed in reactions with non-carbonyl-containing metal halides for the preparation of bimetallic ketene complexes.[18] The reaction of metallaenolates and metal carbonyl electrophiles was therefore a promising route toward μ-malonyl complexes. Our initial efforts with iron enolate **6** and $(CO)_5Re(OSO_2CF_3)$ appeared, by ^1H NMR spectroscopy of the crude reaction mixture, to give malonyl complexes that

(10) Chaudhari, F. M.; Knox, G. R.; Pauson, P. L. *J. Chem. Soc. C* **1967**, 2255.
(11) Blake, D. M.; Vinson, A.; Rye, R. *J. Organomet. Chem.* **1981**, *204*, 257.
(12) Galamb, V.; Pályi, G.; Cser, F.; Furmanova, M. G.; Struchkov, Y. T. *J. Organomet. Chem.* **1981**, *209*, 183.
(13) Bodnar, T. W.; Crawford, E. J.; Cutler, A. R. *Organometallics* **1986**, *5*, 947.
(14) Akita, M.; Kondoh, A. *J. Organomet. Chem.* **1986**, *299*, 369. Akita, M.; Kondoh, A.; Kawahara, T.; Takagi, T.; Moro-oku, Y. *Organometallics* **1988**, *7*, 366.
(15) Schulze, W.; Hartl, H.; Seppelt, K. *Angew. Chem., Int. Ed. Engl.* **1986**, *25*, 185.
(16) Forschner, T. C.; Cutler, A. R. *Organometallics* **1985**, *4*, 1247.
(17) (a) O'Connor, J. M.; Uhrhammer, R.; Rheingold, A. L. *Organometallics* **1987**, *6*, 1987. (b) The numbering system employed here is consistent with Chemical Abstracts nomenclature. See registry numbers in ref 17a as a guide for the nomenclature. (c) The ν(CO) band for **14** was too weak to be unambiguously assigned.
(18) For the use of metallaenolates for preparation of bimetallic ketene complexes, see: (a) Ho, S. C. H.; Straus, D. A.; Armantrout, J.; Schaefer, W. P.; Grubbs, R. H. *J. Am. Chem. Soc.* **1984**, *106*, 2210. (b) Weinstock, I.; Floriani, C.; Chiesi-Villa, A.; Guastini, C. *J. Am. Chem. Soc.* **1986**, *108*, 8298. (c) Reference 14.

Scheme II

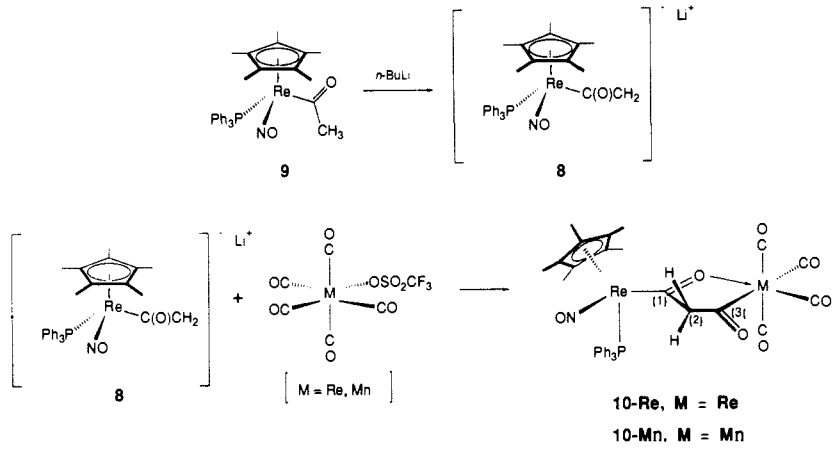

proved too unstable for isolation.[19] We therefore turned to the related rhenium enolate reported in 1986 by Gladysz.[20] The desired rhenaenolate $[(\eta^5\text{-}C_5Me_5)(NO)(PPh_3)Re(COCH_2)]^-Li^+$ (**8**) was generated in tetrahydrofuran solution from $(\eta^5\text{-}C_5Me_5)(NO)(PPh_3)Re(COCH_3)$ (**9**) (1.71 mmol) and *n*-BuLi at −76 °C.[20] The cold enolate solution was then introduced by cannulae into a −76 °C tetrahydrofuran solution of $(CO)_5Re(OSO_2CF_3)$ (1.71 mmol), and the reaction mixture was slowly warmed to room temperature. Workup of the reaction mixture led to isolation of the μ-malonyl complex $(\eta^5\text{-}C_5Me_5)(NO)(PPh_3)Re[\mu\text{-}(COCH_2CO)\text{-}C^1{:}C^3,O^1]Re(CO)_4$ (**10-Re**) as a yellow, air-stable solid in 71% yield. In a similar fashion, reaction of enolate **8** and $(CO)_5Mn(OSO_2CF_3)$ led to isolation of **10-Mn**, as a yellow, air-stable solid in 48% yield (Scheme II).[17a] Both **10-Re** and **10-Mn** were soluble in CH_2Cl_2 and $CHCl_3$, slightly soluble in THF, and insoluble in ether, benzene, toluene, acetonitrile, and acetone.

The spectroscopic properties of **10-Re** and **10-Mn** are similar (Table I). Both complexes exhibited an AB pattern in the ^1H NMR spectrum ($CDCl_3$) with a large geminal coupling constant, the magnitude of which is diagnostic of the 5-membered chelate ring: δ 3.13 (d, J = 20.7 Hz), 2.48 (d, J = 20.7 Hz) for **10-Re** and δ 3.39 (d, J = 20.6 Hz), 2.81 (d, J = 20.6 Hz) for **10-Mn**. In the $^{13}C\{^1H\}$NMR spectra, both complexes exhibited four distinct terminal carbonyl carbon resonances due to the diastereotopic nature of the mutually trans carbonyl ligands. In addition, downfield resonances assigned to the carbonyl carbons of the malonyl ligand were observed at 298.8 (d, J = 7.4 Hz) and 275.6 ppm for **10-Re** and at 283.2 (d, J = 10.0 Hz) and 282.3 ppm for **10-Mn**. In the IR spectrum (CH_2Cl_2) of **10-Re**, bands were observed at 1664 [m, ν(NO)] and 1615 [m, $\nu(C^3{=}O)$, malonyl] cm^{-1}. In order to unambiguously assign $\nu(C^1{=}O)$ of the malonyl ligand, the synthesis of the ^{13}C-enriched complex $(\eta^5\text{-}C_5Me_5)(NO)(PPh_3)Re[\mu\text{-}(^{13}COCH_2CO)\text{-}C^1{:}C^3,O^1]Re(CO)_4$ (**10-^{13}C-O-Re**) was undertaken. The known alkyl complex $(\eta^5\text{-}C_5Me_5)(NO)(PPh_3)Re(CH_3)$ was treated with HBF_4 and ^{13}CO gas to give the labeled carbonyl complex $[(\eta^5\text{-}C_5Me_5)(NO)(PPh_3)Re(^{13}CO)]^+BF_4^-$ (**11-^{13}CO**).[21] Complex **11-^{13}CO** was then carried on to the labeled acyl complex $(\eta^5\text{-}C_5Me_5)(NO)(PPh_3)Re(^{13}COCH_3)$ (**9-^{13}CO**) by the two-step literature procedure for the unlabeled analogue.[20] Acyl **9-^{13}CO** was then used in the preparation of **10-^{13}CO-Re** as described above for the unlabeled isomer. In the IR spectrum, the 1394- and 1374-cm^{-1} bands for **10-Re** were shifted to 1365 and 1336 cm^{-1} for **10-^{13}CO-Re**. Thus, we assign the 1394- and/or 1374-cm^{-1} bands to $\nu(C^1{=}O)$ of the malonyl ligand.

2. X-ray Structure of $(\eta^5\text{-}C_5Me_5)(NO)(PPh_3)Re[\mu\text{-}(COCH_2CO)\text{-}C^1{:}C^3,O^1]Re(CO)_4$ (10-Re). X-ray data were acquired on a pale-yellow crystal of **10-Re** obtained by slow diffusion of pentane into a methylene chloride solution of **10-Re** at −15 °C (Table II). Refinement, described in the Experimental Section, gave the structure shown in Figure 1. Bond distances and bond angles are summarized in Table III. The coordination about Re(1) deviates from ideal octrahedral geometry due to a O(6)–Re(1)–C(5) angle constrained to 76.9 (2)° by the malonyl chelate ring. The C(2)–Re(1)–C(3) angle is opened up to 95.5 (3)°, and the mutually trans carbonyl ligands are bent away from the malonyl ligand with a C(1)–Re(1)–C(4) angle of 174.1 (3)°. The maximum deviations from planarity in the Re(1), O(6), C(7), C(6), C(5) oxametallacycle are at C(5), −0.107 Å, and at C(6), +0.111 Å. The methylene hydrogens on C(6) were not observed and their ideal positions were therefore calculated. The pucker of C(6) away from the bulky PPh_3 ligand places the hydrogen exo to the PPh_3 ligand in a pseudoaxial position, with an H(exo)–C(6)–C(7)–O(6) torsion angle of −107°. The endo hydrogen occupies a pseudoequatorial position with an H(endo)–C(6)–C(7)–O(6) torsion angle of 134°. The nitrosyl ligand is linear, with a Re–N–O angle of 172.0°. The ON–Re(2)–C(7)–O(6) torsion angle (θ) is 178.6°, which places the acyl carbonyl anti to the nitrosyl ligand as predicted by Hückel MO calculations performed by Gladysz on mononuclear rhenium–acyl analogues similar to complex **12**.[22] The θ value observed in **10-Re** is nearly identical in magnitude with that observed in the structure of **10-Mn**.[17] The conformation with θ = 180° is one in which the bulky PPh_3 ligand effectively shields one face of the five-membered chelate ring. The Re(1)–C(5) distance of 2.147 (6) Å is significantly longer than the Re(2)–C(7) distance of 2.048 (5) Å,

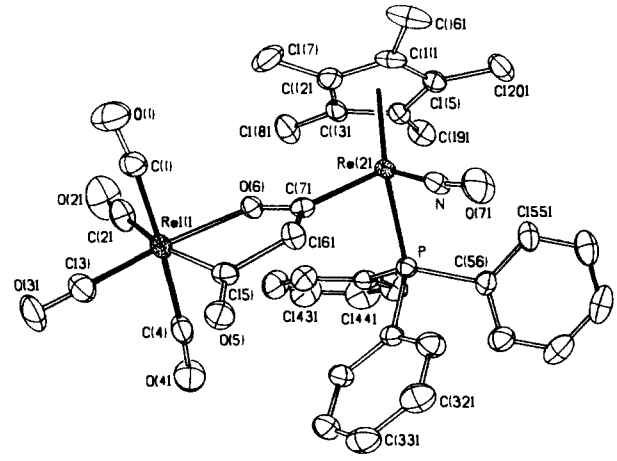

Figure 1. Structure of the bimetallic μ-malonyl complex $(\eta^5\text{-}C_5Me_5)(NO)(PPh_3)Re[\mu\text{-}(COCH_2CO)\text{-}C^1{:}C^3,O^1]Re(CO)_4$ (**10-Re**).

(19) O'Connor, J. M.; Uhrhammer, R. Unpublished observations.
(20) Heah, P. C.; Patton, A. T.; Gladysz, J. A. *J. Am. Chem. Soc.* **1986**, *108*, 1185.
(21) Fernández, J. M.; Gladysz, J. A. *Organometallics* **1989**, *8*, 207.
(22) Bodner, G. S.; Smith, D. E.; Hatton, W. G.; Heah, P. C.; Georgiou, S.; Rheingold, A. L.; Geib, S. J.; Hutchinson, J. P.; Gladysz, J. A. *J. Am. Chem. Soc.* **1987**, *109*, 7688.

Table I. Spectroscopic Characterization of Bimetallic μ-Malonyl Complexes **10**, **17**, **18**, **19**

complex	^{1}H NMR, δ	^{13}C{^{1}H} NMR, ppm	IR, cm^{-1}
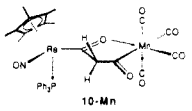 **10-Mn**	1.74 [s, $C_5(CH_3)_5$][b] 2.81 (d, J = 20.6 Hz, -C*H*H-) 3.39 (d, J = 20.6 Hz, -CH*H*-) 7.46, 7.33 (br s, $3C_6H_5$)	283.2 (t, J = 10.0 Hz, Re*C*OCH$_2$-)[f] 282.8 (Mn *C*OCH$_2$-) 219.4 (Mn *C*O) 216.1 (Mn *C*O) 212.6 (Mn *C*O) 211.8 (Mn *C*O) 90.3 (-CO*C*H$_2$CO-)	2060 (m)[f] 1954 (vs) 1924 (s) 1650 [s, ν(NO)] 1632 [s, ν(C^3=O)] 1410 [m, ν(C^1=O)] 1375 [w, ν(C^1=O)]
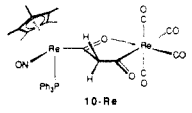 **10-Re**	1.75 [s, $C_5(CH_3)_5$] 2.84 (d, J = 20.7 Hz, -C*H*H-) 3.13 (d, J - 20.7 Hz, -CH*H*-) 7.43, 7.30 (br s, $3C_6H_5$)	289.8 [d, J = 7.4 Hz, Re*C*^{1}OCH$_2$-] 275.6 [Re*C*^{3}OCH$_2$-] 194.9 (Re*C*O) 191.6 (Re*C*O) 191.4 (Re*C*O) 190.9 (Re*C*O) 95.7 (-CO*C*H$_2$CO-)	2080 (w)[f] 1972 (s) 1923 (s) 1664 [m, ν(NO)] 1615 [w, ν(C^1=O)] 1480 (w) 1432 (w) 1394 [w, ν(C^3=O)] 1374 [w, ν(C^3=O)] 1344 (w)
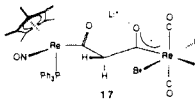 **17**	1.70 [s, $C_5(CH_3)_5$][d] 1.93 (d, J = 15.2 Hz, -C*H*H-) 5.82 (d, J = 15.1 Hz, -CH*H*-) 7.40 (m, $3C_6H_5$)	270.8 [d, J = 9.5 Hz, (Re*C*^{1}OCH$_2$-][d] 270.7 [Re*C*^{3}OCH$_2$-] 190.6 (Re*C*O) 190.2 (Re*C*O) 189.5 (Re*C*O) 189.4 (Re*C*O) 97.0 (-CO*C*H$_2$CO-)	2085 (m)[f] 1985 (vs) 1910 (s) 1648 [m, ν(NO)] 1560 [m, ν(C^3=O)] 1482 [w, ν(C^1=O)] 1467 (m) 1460 (m) 1434 (w)
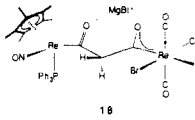 **18**	1.73 [s, $C_5(CH_3)_5$][c] 2.58 (d, J = 15.9 Hz, -C*H*H-) 6.42 (d, J - 15.9 Hz, -CH*H*-) 7.42 (m, $3C_6H_5$)	283.1 [Re*C*^{3}OCH$_2$-][c] 273.1 [d, J = 7.3 Hz, Re*C*^{1}OCH$_2$-] 189.7 (Re*C*O) 189.6 (Re*C*O) 189.5 (Re*C*O) 188.7 (Re*C*O) 97.0 (-CO*C*H$_2$CO-)	2102 (m)[f] 2005 (vs) 1941 (s) 1661 [m, ν(NO)] 1479 (w) 1440 (m) 1377 (w)
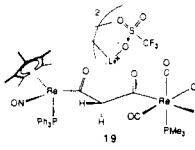 **19**	1.48 (d, J = 14.6 Hz, -C*H*H-) 1.60 [d, J = 9.4 Hz, -P(C*H*$_3$)$_3$] 1.72 [s, $C_5(CH_3)_5$] 5.18 (d, J = 14.7 Hz, -CH*H*-) 7.42 (m, $3C_6H_5$)	262.2 (m, Re*C*OCH$_2$-) 261.6 (m, Re*C*OCH$_2$-) 189.1 (d, J = 10.4 Hz, Re*C*O) 188.7 (d, J = 4.6 Hz, Re*C*O) 188.0 (d, J = 9.6 Hz, Re*C*O) 120.2 (m, J = 318.8 Hz, -*C*F$_3$) 98.4 (-CO*C*H$_2$CO-) 17.9 [d, J = 34.1 Hz, P(*C*H$_3$)$_3$]	2092 (m)[g] 2000 (s) 1980 (vs) 1960 (s) 1646 [s, ν(NO)] 1570 [m, ν(C^3=O)] 1500 [vw, ν(C^3=O)] 1485 (w) 1460 (vw) 1436 (w) 1432 (w)

[a] ^{1}H NMR spectra were recorded at 300 MHz in $CDCl_3$ (unless otherwise noted) at ambient probe temperature and were referenced to the residual solvent resonance. [b] CD_2Cl_2. [c] THF-d_8. [d] CD_2Cl_2, TMEDA. [e] CH_2Cl_2, TMEDA. [f] CH_2Cl_2. [g] $CHCl_3$. [h] ^{13}C NMR were recorded at 75 MHz in $CDCl_3$ (unless otherwise noted) at ambient probe temperature and were referenced to the solvent resonance.

Chart I

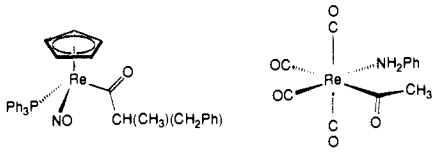

12 13

consistent with a relatively long C(7)–O(6) bond distance 1.286 (6) Å and a shorter C(5)–O(5) distance of 1.232 (9) Å. The difference in Re–acyl bond distance at the two metal centers in **10-Re** is not entirely due to coordination of one of the acyl oxygens to rhenium, as can be seen by a comparison of rhenium–acyl bond distances in $(\eta^5\text{-}C_5H_5)(NO)(PPh_3)Re[C(=O)CHCH_3CH_2Ph]$ (**12**) and $(CO)_4(NH_2Ph)Re[C(=O)CH_3]$ (**13**), for which the rhenium–carbon distances are 2.081 (7)[23] and 2.211 (6) Å,[24] respectively. For comparison, the carbene rhenium–carbon bond distance in $[(\eta^5\text{-}C_5H_5)(NO)(PPh_3)Re(=CHPh)]^+PF_6^-$ is 1.949 (6) Å.[25]

(23) Bodner, G. S.; Patton, A. T.; Smith, D. E.; Georgiou, S.; Tam, W.; Wong, W.-K.; Strouse, C. E.; Gladysz, J. A. *Organometallics* **1987**, *6*, 1954.
(24) Lukehart, C. M.; Zeile, J. V. *J. Organomet. Chem.* **1977**, *140*, 309.

Scheme III

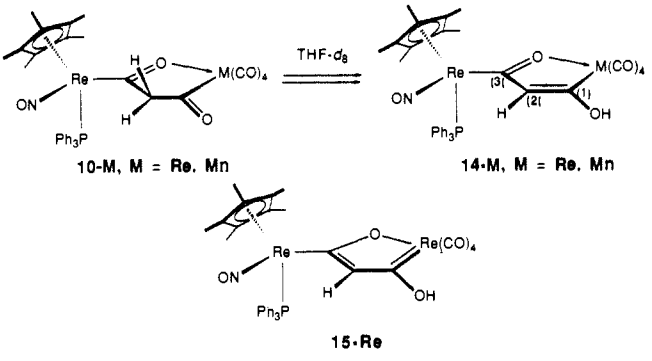

10-M, M = Re, Mn 14-M, M = Re, Mn 15-Re

3. Keto–Enol Tautomerization in 10-Re and 10-Mn. In THF-d_8 solution the ^{1}H NMR spectrum of **10-Re** exhibits three new resonances at δ 6.28 (1 H), 8.91 (1 H), and 1.73 (15 H), in addition to resonances for **10-Re** at 1.76 (s, 15 H, C_5Me_5), 2.47 (d, J = 20.5 Hz, 1 H, -C*H*H-), 3.01 (d, J = 20.5 Hz, 1 H, -CH*H*-), and 7.4–7.9 [br, -C_6H_5]. We attribute these new

(25) Kiel, W. A.; Lin, G.-Y.; Constable, A. G.; McCormick, F. B.; Strouse, C. E.; Eisenstein, O.; Gladysz, J. A. *J. Am. Chem. Soc.* **1982**, *104*, 4865.

Table II. Crystal and Data Collection and Refinement Parameters for **10-Re**, **17-TMEDA**, and **19**

	10-Re	**17-TMEDA**	**19**
formula	$C_{35}H_{32}NO_7PRe_2$	$C_{41}H_{48}LiN_3O_7PBrRe_2 \cdot C_4H_8Cl_4$	$C_{39}F_3H_{41}LiNO_{10}P_2Re_2S$
lattice type	triclinic	monoclinic	monoclinic
space group	$P\bar{1}$	$P2_1/n$	$C2/c$
a, Å	10.5112 (11)	10.977 (5)	18.269 (3)
b, Å	11.0281 (17)	28.094 (15)	22.622 (3)
c, Å	16.7597 (22)	17.204 (8)	22.903 (4)
α, deg	74.860 (9)		
β, deg	83.512 (8)	95.73 (4)	100.01 (1)
γ, deg	68.508 (8)		
V, Å^3	1744.7 (4)	5279 (5)	9322 (3)
Z	2	4	8
cryst dimens, mm	0.16 × 0.18 × 0.22	0.31 × 0.39 × 0.75	0.24 × 0.24 × 0.30
cryst color	yellow	yellow	orange
D(calc), g/cm^3	1.87	1.74	1.73
μ(Mo Kα), cm^{-1}	74.19	56.75	56.6
temp, °C	23	−100	23
T(max)/T(min)	0.431/0.323	0.1799/0.2605	0.104/0.081
radiation type	Mo Kα (λ = 0.71073 Å)	Mo Kα (λ = 0.71073 Å)	Mo Kα (λ = 0.71073 Å)
2θ range, deg	4–56	4–45	4–52
no. of read data	8708	6079	7436
no. of unique data	8425	5715	7043
no. of unique obsd data	6994 ($5\sigma(F_o)$)	3793 ($6.0\sigma(F_o)$)	4697 ($5\sigma(F_o)$)
$R(F)$, %	3.00	6.22	4.53
$R(wF)$, %	3.92	8.82	4.92
GOF	1.044	2.12	1.027
$\Delta(\rho)$, e Å^{-3}	1.24	1.49	3.27

Table III. Selected Bond Distances and Angles for **10-Re**

(a) Bond Distances (Å)

A–B	distance	A–B	distance
Re(1)–C(1)	1.991 (6)	O(6)–C(7)	1.286 (6)
Re(1)–C(2)	2.004 (8)	C(6)–C(7)	1.516 (9)
Re(1)–C(3)	1.918 (6)	C(5)–C(6)	1.549 (7)
Re(1)–C(4)	2.004 (7)	N–O(7)	1.211 (7)
Re(1)–C(5)	2.147 (6)	C(1)–O(1)	1.415 (8)
Re(1)–O(6)	2.164 (3)	C(2)–O(2)	1.120 (11)
Re(2)–CNT[a]	1.990 (7)	C(3)–O(3)	1.146 (8)
Re(2)–P	2.393 (1)	C(4)–O(4)	1.130 (9)
Re(2)–N	1.757 (5)	C(5)–O(5)	1.232 (9)
Re(2)–C(7)	2.048 (5)		

(b) Bond Angles (deg)

A–B–C	angle	A–B–C	angle
C(1)–Re(1)–C(2)	89.9 (3)	CNT–Re(2)–P	127.8 (1)
C(1)–Re(1)–C(3)	87.6 (3)	CNT–Re(2)–N	124.7 (2)
C(1)–Re(1)–C(4)	174.1 (3)	CNT–Re(2)–C(7)	117.8 (3)
C(1)–Re(1)–C(5)	90.5 (2)	N–Re(2)–P	92.3 (2)
C(1)–Re(1)–O(6)	92.8 (2)	N–Re(2)–C(7)	97.6 (2)
C(2)–Re(1)–C(3)	95.5 (3)	P–Re(2)–C(7)	87.5 (1)
C(2)–Re(1)–C(4)	92.5 (3)	Re(2)–C(7)–O(6)	121.9 (4)
C(2)–Re(1)–C(5)	168.1 (2)	Re(2)–C(7)–C(6)	123.6 (3)
C(2)–Re(1)–O(6)	91.2 (2)	C(6)–C(7)–O(6)	114.3 (4)
C(3)–Re(1)–C(4)	86.8 (3)	C(5)–C(6)–C(7)	113.0 (4)
C(3)–Re(1)–C(5)	96.4 (3)	Re(1)–O(6)–C(7)	121.5 (4)
C(3)–Re(1)–O(6)	173.3 (2)	Re(1)–C(5)–O(5)	131.9 (4)
C(4)–Re(1)–C(5)	88.3 (2)	Re(1)–C(5)–C(6)	111.8 (4)
C(4)–Re(1)–O(6)	92.5 (2)	O(5)–C(5)–C(6)	116.4 (5)
C(5)–Re(1)–O(6)	76.9 (2)	Re(2)–N–O(7)	172.0 (5)

[a] CNT = centroid of the Cp* ring.

resonances to the enol tautomer (η^5-C_5Me_5)(NO)(PPh_3)Re{μ-[COCH=C(OH)]-C^1,O^3:C^3}Re(CO)$_4$ (**14-Re**, Scheme III).[5,17b,c] The intensity ratio of the ^{1}H NMR resonance at δ 6.28 (**12-Re**) to that at 3.01 (**10-Re**) was temperature dependent with $K_{eq}^{23°C}$ = [**14-Re**]/[**10-Re**] = 0.66. When the THF-d_8 solvent was replaced with chloroform-d, the ^{1}H NMR spectrum again indicated only the presence of **10-Re**. The existence of two species in THF-d_8 solution was supported by the obervation of two resonances in the ^{31}P{^{1}H} NMR spectrum at δ 19.3 and 22.7 in approximately a 2:1 ratio. In the ^{13}C{^{1}H} NMR spectrum a resonance at 225.4 ppm was assigned to the carbon bearing the hydroxyl group. This chemical shift may indicate some carbenoid resonance contribution; as shown in **15-Re** (Scheme III), however, a dominant

Chart II

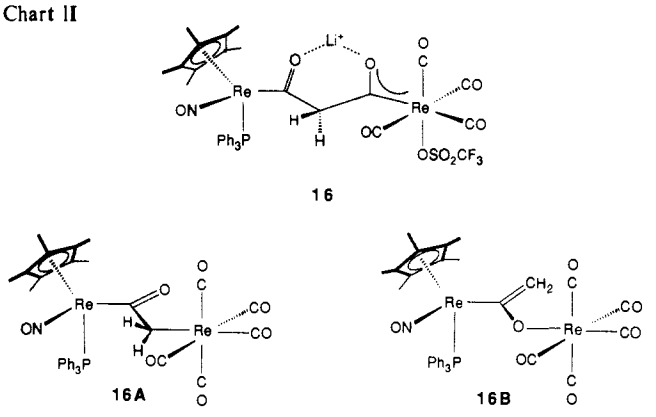

ground-state structure of this type would exhibit a carbene carbon atom chemical shift below 300 ppm.[26] In contrast to **10-Re**, the manganese analogue, **10-Mn**, exhibited no spectroscopic evidence for an enol tautomer in THF solution ($K_{eq}^{23°C}$ = [**14-Mn**]/[**10-Mn**] < 0.02). However, enolization also appeared to be operative in **10-Mn** as indicated by incorporation of deuterium into the methylene hydrogen sites upon addition of D_2O to a THF solution of **10-Mn**.[5,27]

4. Mechanism of μ-Malonyl Complex Formation. When the reaction between enolate anion **8** and (CO)$_5$Re(OSO$_2$CF$_3$) was monitored by ^{31}P{^{1}H} NMR spectroscopy, an intermediate species was observed at low temperature. Addition of 1 equiv of n-BuLi to an orange THF-d_8 solution of acyl complex **9** at −76 °C resulted in a deep red solution. In the ^{31}P{^{1}H} NMR spectrum of this reaction mixture, the original resonance at δ 19.9 (for **9**) was replaced by new resonances at 28.8 and 22.9,[28] corresponding to enolate **8**. Addition of a THF solution of (CO)$_5$Re(OSO$_2$CF$_3$) to this deep red solution at −76 °C, resulted in an orange solution, for which the ^{31}P{^{1}H} NMR spectrum exhibited a single resonance at δ 17.9. When the reaction mixture was warmed to room temperature the δ 17.9 resonance was replaced by new resonances at δ 19.3 and 22.7, corresponding to **10-Re** and **14-Re**, respectively.

(26) Darst, K. P.; Lenhert, P. G.; Lukehart, C. M.; Warfield, L. T. *J. Organomet. Chem.* **1980**, *195*, 317.

(27) O'Connor, J. M.; Uhrhammer, R.; Rheingold, A. L. Manuscript in preparation.

(28) The observation of two mononuclear enolate species at low temperature corresponding to **8** may be due to conformational isomers or different lithium ion aggregates.

Scheme IV

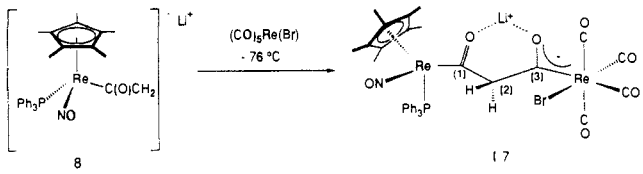

Three reasonable structures for the low-temperature intermediate (δ 17.9) are as follows: (a) the anionic μ-malonyl complex, **16**, which would result from direct attack of the enolate carbon at a carbon monoxide ligand; (b) the neutral μ-ketene-(C:C) complex, **16A**, from displacement of triflate by the enolate carbon; and (c) the neutral μ-ketene-(C:O), **16B**, from displacement of triflate by the enolate oxygen (Chart II). Formation of **10-Re** from intermediate **16** requires loss of triflate anion and coordination of the malonyl oxygen. Conversion of **16A** to **10-Re** requires a migratory CO insertion.[29] In the case of intermediate **16B**, an intramolecular rearrangement must occur to generate **10-Re**.

To further distinguish between structures **16**, **16A**, and **16B**, an additional experiment was performed in which ^{1}H and ^{13}C{^{1}H} NMR spectra of the intermediate were obtained at −80 °C. In the ^{1}H NMR spectrum a doublet assigned to one of the malonyl hydrogens was observed at δ 5.58 (J = 16 Hz), indicative of a lithium-chelated malonyl complex (vide infra, compound **17**). In the ^{13}C NMR spectrum, two downfield resonances were observed at 271.6 and 267.5 ppm, which are consistent with structure **16** and inconsistent with **16A** and **16B**. ^{31}P NMR spectra taken immediately before and after the ^{13}C NMR spectrum, indicated that only minor decomposition had occurred over the course of the experiment.

5. Synthesis of an Anionic μ-Malonyl Complex, {(η^5-C_5Me_5)(NO)(PPh_3)Re[μ-($COCH_2CO$)-C^1:C^3]Re(CO)$_4$(Br)}$^-$Li$^+$ (17). Additional, circumstantial support for the structure of intermediate **16** was obtained from the reaction of enolate **8** and (CO)$_5$ReBr. Reaction of **8** with (CO)$_5$ReBr at −76 °C led to isolation of a new anionic malonyl complex, {(η^5-C_5Me_5)(NO)(PPh_3)Re[μ-($COCH_2CO$)-C^1:C^3]Re(CO)$_4$(Br)}$^-$Li$^+$ (**17**), as a yellow solid in good to excellent yields (70–90%, Scheme IV). When the reaction of **8** and (CO)$_5$ReBr was followed at low temperature by ^{31}P NMR, no intermediates were observed and **17** appeared to be formed directly at −76 °C. Complex **17** is air-stable in the solid state but air-sensitive in solution. In the ^{1}H NMR spectrum (THF-d_8) of **17**, a downfield doublet at δ 5.90 (J = 15.6 Hz, 1 H) and an upfield doublet at δ 1.92 (J = 15.6 Hz, 1 H) were assigned to the methylene hydrogens of the malonyl ligand. The assignment was confirmed by ^{1}H NMR decoupling experiments. Addition of one or more equivalents of TMEDA to suspensions of **17** in organic solvents greatly enhanced solubility and facilitated characterization as the TMEDA adduct. In the ^{13}C NMR spectrum (CD_2Cl_2, TMEDA, 14 °C) the methylene carbon resonance was observed at 97.0 ppm as a doublet of doublets (J = 138.1, 120.8 Hz). From NMR selective-heteronuclear-decoupling experiments it was determined that the larger one-bond coupling to carbon was to the downfield methylene hydrogen. For comparison, $^1J_{CH(eq)}$ = 126.4 and $^1J_{CH(ax)}$ = 122.4 in cyclohexane.[30] Four terminal carbonyl carbon resonances were observed between 190.6 and 189.4 ppm, and two acyl carbon resonances were observed at 270.7 and 270.8 (d, J = 9.5 Hz) ppm. In the IR spectrum (CH_2Cl_2, TMEDA) of **17**, three ν(CO) bands were observed at 2085 (m), 1985 (vs), and 1910 cm^{-1}. Only one band was observed in the acyl region, at 1560 cm^{-1}.

In order to clarify the ambiguous IR spectroscopic data on **17** we prepared the carbon-13 enriched malonyl complexes **17-^{13}CO-A** and **17-^{13}CO-B** from the labeled precursors **9-^{13}CO** and (^{13}CO)$_5$ReBr, respectively (Chart III). **9-^{13}CO** was prepared as described above and (^{13}CO)$_5$ReBr was prepared (with 67% isotopic enrichment in cis carbonyl sites)[31] by ligand exchange in (CO)$_5$Re(Br) with ^{13}CO gas. In the IR spectrum (CH_2Cl_2, TMEDA) of **17-^{13}CO-A**, a band at 1482 cm^{-1} was greatly diminished in relative intensity from the same band in the unlabeled complex, and we therefore assigned this band to the carbonyl bonded to the chiral rhenium center, ν(C^1=O). We were unable to determine if a new band was present at ~1450 cm^{-1}, as that region was obscured by other bands. For comparison, the acyl stretching frequency in the mononuclear acyl **9** was observed at 1555 cm^{-1}. In the ^{13}C NMR spectrum (CD_2Cl_2, TMEDA) of **17-^{13}CO-A**, the labeled carbon was observed as a doublet of doublets at 270.8 ppm (J_{CP} = 9.6 Hz, J_{CH} = 5.1 Hz). Only one of the methylene hydrogens is therefore coupled to the carbonyl carbon. This was confirmed in the ^{1}H NMR spectrum (CD_2Cl_2) where the upfield methylene resonance at δ 1.93 was observed as a doublet of doublets ($^2J_{HH}$ = 15.6 Hz, $^2J_{CH}$ = 5.1 Hz), but the downfield methylene resonance at δ 5.81 was observed as a simple doublet ($^2J_{HH}$ = 15.6 Hz, $^2J_{CH}$ < 1 Hz).

In the IR spectrum (CH_2Cl_2, TMEDA) of **17-^{13}CO-B**, a new band was observed at 1527 cm^{-1} and the band at 1560 cm^{-1} was greatly diminished in relative intensity when compared to the spectrum of the unlabeled complex. In the ^{13}C{^{1}H} NMR spectrum (CD_2Cl_2, TMEDA) of **17-^{13}CO-B** the labeled carbon resonance was observed as a singlet at 270.7 ppm. Once again differential $^2J_{CH}$ coupling was observed between the labeled carbon and the methylene hydrogens in the ^{1}H NMR spectrum, as evidenced by a doublet of doublets at δ 1.93 ($^2J_{HH}$ = 15.2 Hz, $^2J_{CH}$ = 4.8 Hz) and a doublet at δ 5.81 ($^2J_{HH}$ = 15.2 Hz, $^2J_{CH}$ < 1 Hz).

6. X-ray Structure of [(η^5-C_5Me_5)Re(NO)(PPh_3)Re[μ-($COCH_2CO$)-C^1:C^3]Re(CO)$_4$(Br)]$^-$Li$^+$ (17). X-ray data were acquired on a pale-yellow crystal of the TMEDA adduct of **17** obtained by slow addition of dibutyl ether to a dichloroethane solution of **17**·TMEDA at −15 °C under N_2 gas (Table II).[32]

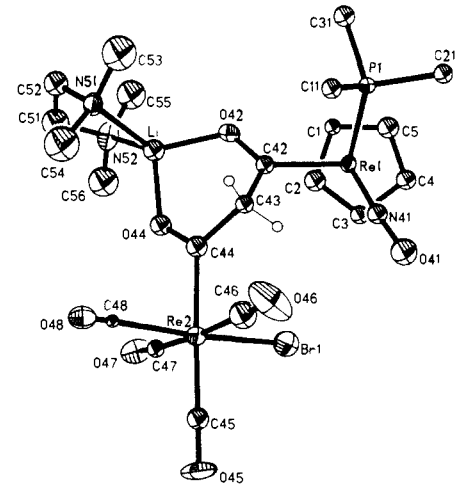

Figure 2. Structure of **17**, showing the orientation of Li$^+$ in relation to the dirhenium backbone; phenyl rings and cyclopentadienyl methyls are omitted.

Chart III

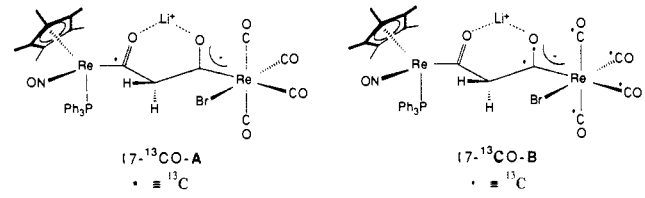

(29) Martin, B. D.; Warner, K. E.; Norton, J. R. *J. Am. Chem. Soc.* **1986**, *108*, 33 and references therein.

(30) Chertkov, V. A.; Sergeyev, N. M. *J. Am. Chem. Soc.* **1977**, *99*, 6750.

(31) The degree of ^{13}CO enrichment was determined at the malonyl complex stage [(η^5-C_5Me_5)(NO)(PPh_3)Re[μ-($COCH_2{}^{13}CO$)-C^1:C^3,O^1]Re(^{13}CO)$_4$ by measuring the relative integral heights of the ^{1}H NMR resonances (one of the methylene hydrogens) for the unlabeled isomer (a doublet) and the corresponding carbon-13 labeled isomer (a doublet of doublets): δ 3.13 (dd, $^2J_{HH}$ = 20.6 Hz, $^2J_{CH}$ = 4.4 Hz), 2.49 (dd, $^2J_{HH}$ = 20.6 Hz, $^2J_{CH}$ = 4.7 Hz), 3.13 (d, $^2J_{HH}$ = 20.6 Hz), 2.49 (d, $^2J_{HH}$ = 20.6 Hz).

(32) Structural determination carried out at the UCSD X-ray Crystallographic Facility.

Scheme V

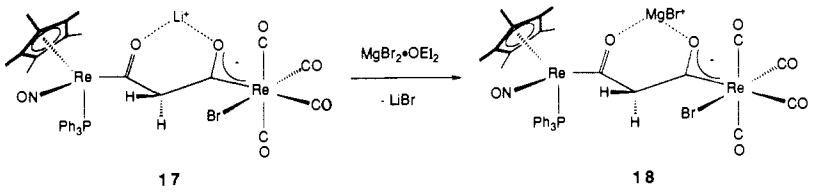

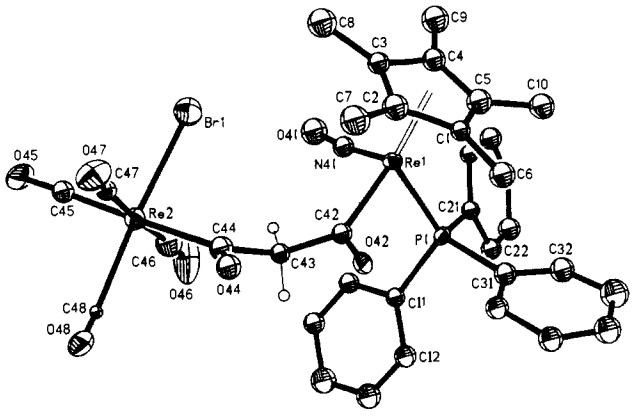

Figure 3. Structure of **17** with the Li·TMEDA fragment omitted.

Because crystal decomposition was rapid, even in a sealed capillary at room temperature, the data were collected at −100 °C. The intensities of three monitor reflections measured after every 100 reflections decayed by ca. 15% during 65 h of X-ray exposure. Refinement, described in the Experimental Section, gave the structure shown in Figures 2 and 3. Bond distances and bond angles are summarized in Table IV. Figure 2 shows the three malonyl carbon atoms C(42), C(43), and C(44) bridging the two metal centers Re(1) and Re(2) and the orientation of the Li^+-TMEDA unit in relation to the dirhenium backbone. The lithium ion is bonded to both malonyl oxygens O(42) and O(44) to form a six-membered ring containing Li,O(42),C(42),C(43),C(44),O-(44). The chelate ring adopts a slightly twisted boat conformation with the methylene carbon C(43) and lithium atom both puckered upwards. The coordination about the lithium ion is a distorted tetrahedral geometry. The malonyl oxygens are coordinated to lithium with an O(42)-Li-O(44) bond angle of 92.6°, and the TMEDA nitrogens coordinate to lithium with a N(51)-Li-N(52) bond angle of 87.5°. These angles are much more acute than the N-Li-O bond angles (117.0–126.4°). Both rhenium atoms exhibit only small deviations from ideal octahedral geometry (bond angles range from 84.4 to 98.3 and from 172.8 to 178.0°). An N-(41)-Re(1)-C(42)-O(42) torsion angle (θ) of 179.6° places the nitrosyl and acyl moieties in an anti relationship. The Re(2)-C(44)-O(44) acyl does not quite eclipse the Re(2)-C(46) or C(47) rhenium carbonyl bonds with C(46)-Re(2)-C(44)-O(44) and C(47)-Re(2)-C(44)-O(44) torsion angles of 155.4 and −27.5°, respectively.[33] The Br-Re(2)-C(44)-O(44) torsion angle is −112.4°. The Re(1)-C(42) bond distance of 2.103 Å and the Re(2)-C(44) bond distance of 2.145 Å are consistent with a distinct degree of carbene character in the rhenium–carbon bonds. Both acyl bond lengths C(42)-O(42) and C(44)-O(44) are significantly elongated at 1.274 and 1.269 Å, respectively, which is consistent with the low-energy stretching frequencies observed for these carbonyls (1482 and 1560 cm^{-1}) in the IR spectrum of **17**.

The conformation of the malonyl ligand in **17** is emphasized in Figure 3. The methylene hydrogen positions H_a and H_b were calculated. H_b occupies an equatorial position, nearly in the plane of both acyls. The H_b-C(43)-C(42)-O(42) and H_b-C(43)-C-(44)-O(44) torsion angles are 179.4 and 162.9°, respectively. H_b is at a 2.55-Å nonbonded distance from the nitrosyl nitrogen N(41). H_a occupies an axial position and is directed towards the C(11)-C(16) phenyl ring, with a nonbonded distance of 3.16 Å from the centroid of that ring. The H_a–C(43)–C(42)–O(42) and H_a-C(43)-C(44)-O(44) torsion angles are 60.9° and 78.7°, respectively.

(33) For a discussion of conformational preferences in octahedral acyl complexes see: Blackburn, B. K.; Davies, S. G.; Sutton, K. H.; Whittaker, M. *Chem. Soc. Rev.* **1988**, *17*, 147.

Table IV. Selected Bond Distances and Angles for **17**

(a) Bond Distances (Å)

A–B	distance	A–B	distance
Re(1)-P(1)	2.370 (6)	O(44)-Li	1.879 (44)
Re(1)-C(42)	2.103 (21)	O(44)-C(44)	1.269 (29)
Re(2)-Br(1)	2.598 (3)	O(45)-C(45)	1.173 (32)
Re(2)-C(44)	2.145 (24)	O(46)-C(46)	1.139 (37)
Re(2)-C(45)	1.892 (25)	O(47)-C(47)	1.053 (30)
Re(2)-C(46)	1.928 (29)	O(48)-C(48)	0.737 (27)
Re(2)-C(47)	2.000 (23)	N(51)-Li	2.094 (41)
Re(2)-C(48)	2.143 (20)	N(52)-Li	2.035 (46)
O(41)-N(41)	1.227 (26)	C(42)-C(43)	1.507 (31)
O(42)-Li	1.868 (44)	C(43)-C(44)	1.563 (32)
O(42)-C(42)	1.274 (27)		

(b) Bond Angles (deg)

A–B–C	angle	A–B–C	angle
P(1)-Re(1)-N(41)	93.4 (6)	Li-O(42)-C(42)	122.4 (19)
P(1)-Re(1)-C(42)	87.4 (6)	Li-O(44)-C(44)	126.3 (19)
N(41)-Re(1)-C(42)	98.3 (9)	Re(1)-N(41)-O(41)	172.7 (15)
Br(1)-Re(2)-C(44)	84.3 (6)	O(42)-Li-O(44)	96.2 (19)
Br(1)-Re(2)-C(45)	93.7 (7)	O(42)-Li-N(51)	118.9 (21)
C(44)-Re(2)-C(45)	178.0 (10)	O(44)-Li-N(51)	112.1 (20)
Br(1)-Re(2)-C(46)	92.1 (8)	O(42)-Li-N(52)	126.4 (22)
C(44)-Re(2)-C(46)	89.1 (11)	O(44)-Li-N(52)	117.0 (21)
C(45)-Re(2)-C(46)	90.7 (12)	N(51)-Li-N(52)	87.5 (17)
Br(1)-Re(2)-C(47)	84.4 (6)	Re(1)-C(42)-O(42)	120.1 (16)
C(44)-Re(2)-C(47)	85.0 (9)	Re(1)-C(42)-C(43)	121.5 (15)
C(45)-Re(2)-C(47)	95.1 (10)	O(42)-C(42)-C(43)	118.3 (18)
C(46)-Re(2)-C(47)	173.4 (11)	C(42)-C(43)-C(44)	114.7 (17)
Br(1)-Re(2)-C(48)	172.8 (7)	Re(2)-C(44)-O(44)	124.9 (17)
C(44)-Re(2)-C(48)	89.5 (9)	Re(2)-C(44)-C(43)	119.2 (15)
C(45)-Re(2)-C(48)	92.5 (9)	O(44)-C(44)-C(43)	115.8 (20)
C(46)-Re(2)-C(48)	91.5 (10)	Re(2)-C(45)-O(45)	178.5 (21)
C(47)-Re(2)-C(48)	91.4 (9)		

7. Exchange of Mg^{+2} with Li^+ in 17. Complex **17** underwent reaction with magnesium bromide in CH_2Cl_2 to give the magnesium-chelated malonyl complex $\{(\eta^5\text{-}C_5Me_5)(NO)(PPh_3)Re[\mu\text{-}(COCH_2CO)\text{-}C^1{:}C^3]Re(CO)_4(Br)\}^-MgBr^+$ (**18**) in quantitative yield by ^1H NMR spectroscopy (57% isolated yield, Scheme V). As was observed for **17**, the ^1H NMR spectrum (THF-d_8) of **18** exhibited two widely separated doublets [δ 6.42 (J = 15.9 Hz) and 2.58 (J = 15.9 Hz)], which were assigned to the diastereotopic methylene hydrogens of the malonyl ligand. In the ^{13}C NMR spectrum (THF-d_8) of **18** the carbonyl resonances of the malonyl ligand were observed at 283.1 and 273.1 (d, J = 7.3 Hz) ppm. In the IR spectrum (CH_2Cl_2), no acyl bands were observed above 1479 cm^{-1}, consistent with chelation of the malonyl oxygens to the strong magnesium Lewis acid. The presence of magnesium and bromide was confirmed by C, H, N, and Br analysis, and a molecular weight determination in CH_2Cl_2 solution was consistent with the indicated structure.

8. Conversion of 17 to 10-Re. Tetrahydrofuran-d_8 solutions of **17** in sealed NMR tubes slowly decomposed over the course of weeks to give a complex mixture of products including small amounts of the chelating malonyl **10-Re**. In the presence of 12-crown-4 in methylene chloride solution, the thermal decomposition of **17** was much cleaner and resulted in the formation

Scheme VI

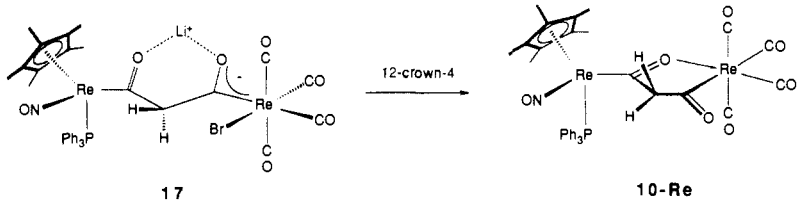

Scheme VII

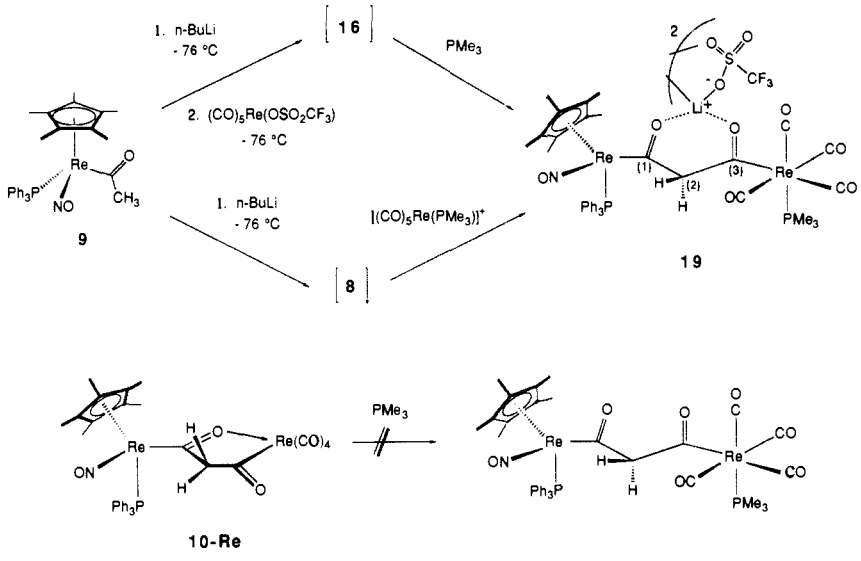

of **10-Re** as the major product. Thus, an NMR tube reaction that employed 0.022 mmol (65.7 mM) of **17** and 2.7 equiv of 12-crown-4 in methylene chloride-d_2 was monitored at 23 °C by ^{1}H NMR spectroscopy (with 1,4-bis(trimethylsilyl)benzene as an internal standard). After 119 h **17** was completely consumed and the product distribution consisted of 77% **19-Re**, 18% acyl **9**, and 9% mononuclear carbonyl **11**.

9. Synthesis of a Neutral μ-Malonyl Complex, {(η^5-C_5Me_5)(NO)(PPh_3)Re[μ-($COCH_2CO$)-C^1:C^3]Re(CO)$_4$(PMe_3)}·$Li^+OSO_2CF_3^-$ (19). In an attempt to trap intermediate **16**, enolate **8** was allowed to react with $(CO)_5Re(OSO_2CF_3)$ at −76 °C, followed by addition of a 40 molar excess of PMe_3 to the reaction mixture at that temperature. After the mixture was warmed to room temperature a 45% yield of the neutral malonyl complex {(η^5-C_5Me_5)(NO)(PPh_3)Re[μ-($COCH_2CO$)-C^1:C^3]Re(CO)$_4$(PMe_3)}·$Li^+OSO_2CF_3^-$ (**19**) was isolated as a yellow crystalline solid (Scheme VII). Complex **19** is air-stable in the solid state over the course of days and slightly air-sensitive in solution. The spectroscopic properties of **19** are very similar to those observed for **17**. In the ^{1}H NMR spectrum ($CDCl_3$) of **19** a large chemical shift difference was observed for the two methylene hydrogens: δ 5.18 (d, J = 14.7 Hz) and 1.48 (d, J = 14.6 Hz). In the $^{13}C\{^1H\}$ NMR spectrum ($CDCl_3$, 14 °C) of **19** three terminal carbonyl ligand carbon resonances at 189.1 (d, J = 14.7 Hz), 188.7 (d, J = 4.6 Hz), and 188.0 (d, J = 9.6 Hz) ppm were assigned to the carbonyl ligands cis to the PMe_3 ligand. A resonance at 188.0 (d, J = 41.0 Hz) ppm was assigned to the carbonyl ligand trans to the PMe_3 ligand. The carbonyl carbon resonances of the malonyl ligand were observed as unresolved multiplets at 262.2 and 261.6 ppm and three lines of the quartet expected for the CF_3 carbon were observed at 120.2 ppm (J = 318.8 Hz). In the IR spectrum ($CHCl_3$) of **19** four bands were observed between 2092 and 1960 cm^{-1}, which were assigned to the terminal CO ligands. A band at 1646 cm^{-1} was assigned to the nitrosyl ligand stretch, a band at 1570 cm^{-1} was assigned to one of the acyl units of the malonyl ligand, and five lower energy, unassigned bands were observed between 1500 and 1432 cm^{-1}.

In order to assign the carbonyl stretching frequencies of the malonyl ligand, the isotopically enriched complexes {(η^5-C_5Me_5)(NO)(PPh_3)Re[μ-($^{13}COCH_2CO$)-C^1:C^3]Re(CO)$_4$(PMe_3)}·$Li^+OSO_2CF_3^-$ (**19-^{13}CO-A**) and {(η^5-C_5Me_5)(NO)(PPh_3)Re[μ-($COCH_2{}^{13}CO$)-C^1:C^3]Re(CO)$_4$(PMe_3)}·$Li^+OSO_2CF_3^-$ (**19-^{13}CO-B**) were prepared from the labeled precursors **9-^{13}CO** and $(^{13}CO)_5Re(OSO_2CF_3)$, respectively. The 1500-cm^{-1} band observed in the unlabeled isomer, **19**, was absent in the spectrum of **19-^{13}CO-A** and therefore was assigned to the malonyl carbonyl [ν(C^1=O)] bonded to the chiral rhenium center in **19**. The 1570-cm^{-1} band observed in the IR spectrum of **19** was shifted to 1539 cm^{-1} in the spectrum of **19-^{13}CO-B** and was assigned to the carbonyl [ν(C^3=O)] bonded to the rhenium bearing the PMe_3 ligand. In the ^{1}H NMR spectrum of **19-^{13}CO-A**, differential $^2J_{CH}$ coupling was observed between the labeled carbon and the methylene hydrogens of the malonyl ligand: δ 1.48 (dd, $^2J_{HH}$ = 14.5 Hz, $^2J_{CH}$ = 5.5 Hz) and 5.18 (d, J_{HH} = 14.5 Hz, $^2J_{CH}$ = 0 Hz). In the ^{1}H NMR spectrum of **19-^{13}CO-B** the δ 1.48 resonance appeared as a broad doublet (J_{HH} = 15.4 Hz) with unresolved $^2J_{CH}$ coupling ($\omega_{1/2}$ > 5 Hz), and the downfield resonance at δ 5.18 appeared as a simple doublet (J_{HH} = 14.9 Hz) of normal line width.

Complex **19** was independently prepared by reaction of enolate **8** and $[(CO)_5Re(PMe_3)]^+OSO_2CF_3^-$ in 42% yield. Complex **10-Re** is also a potential precursor to a non-lithium ion chelated analogue of **19**; however, **10-Re** failed to react with PMe_3 at room temperature (Scheme VII).

When deuterium oxide is added to a chloroform-d solution of **19** under nitrogen gas, a ^{1}H NMR spectrum of the sample indicated complete conversion to a new species with NMR resonances at δ 7.4 (br s, 15 H), 3.96 (d, J = 15.5 Hz, 1 H), 2.72 (d, J = 15.5 Hz, 1 H), 1.70 (s, 15 H), 1.60 (d, J = 9.3 Hz, 9 H). Over the course of hours this new species was converted to the cationic mononuclear carbonyl **11** (70%) and other unidentified species. On the basis of the chemical shift and coupling constants for the methylene hydrogen resonances we propose a nonchelating malonyl structure for this transient species.

10. X-ray Structure of {(η^5-C_5Me_5)(NO)(PPh_3)Re[μ-($COCH_2CO$)-C^1:C^3]Re(CO)$_4$(PMe_3)}·$Li^+OSO_2CF_3^-$ (19). In order to clarify the unusual spectroscopic data and the mode of lithium cation interaction with the transition-metal ligands, an X-ray diffraction study was performed on **19**. Data were acquired on an orange crystal of **19** and refinement, described in the Exper-

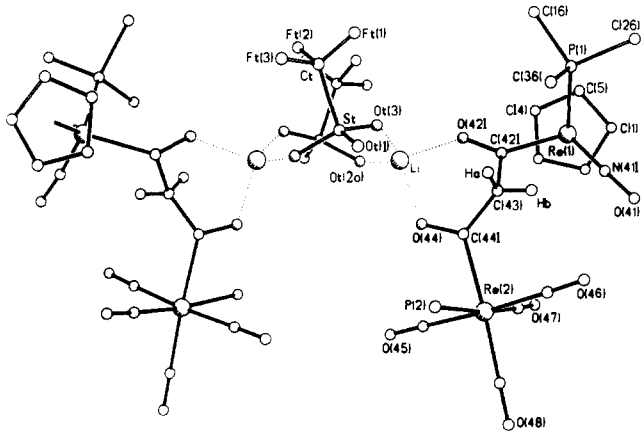

Figure 4. Structure of **19**, showing the orientation of Li in relation to the dirhenium backbone; phenyl rings and cyclopentadienyl methyls omitted.

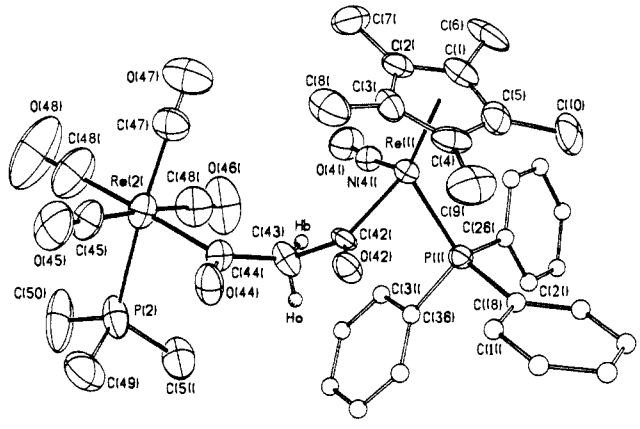

Figure 5. Structure of **19** with $LiOSO_2CF_3$ omitted.

imental Section, gave the structure shown in Figures 4 and 5 (Tables II and V). Figure 4 shows the dimeric solid-state structure of **19** and the orientation of the triflate and lithium ions in relation to the dirhenium backbone of the molecule. The arrangement of oxygen atoms about the lithium is tetrahedral, with two oxygen atoms provided by the malonyl ligand and two triflate ions each providing one oxygen atom. The Li–O(42) and Li–O(44) distances are 1.940 and 1.908 Å, respectively. Two oxygen atoms of each triflate ion bridge two lithium atoms with Ot(3)–Li and Ot(2a)–Li distances of 1.922 and 1.902 Å, respectively. The average oxygen–lithium–oxygen angle is 109.1°, and the bite angle of the malonyl (O(42)–Li–O(44)) is 93.6°. The ON–Re(1)–C(42)–O(42) torsion angle (θ) is 178.5°, which places C(42)–O(42) anti to the NO ligand. The Re(1)–C(42) distance of 2.069 Å is significantly shorter than the 2.194 Å Re(2)–C(44) distance.

The conformation of the malonyl ligand is emphasized in Figure 5. The Li, O(42), C(42), C(43), and O(44) atoms form a six-membered ring that exists in a boat conformation, with C(43) puckered toward the PPh_3 ligand. The bridging methylene hydrogens, H_a and H_b, were located on a difference map and refined. H_a is at a 2.88 Å nonbonded distance from both C(35) and C(36) of a phenyl ring on phosphorus and is 2.78 Å from the centroid of that ring. H_a is directed nearly orthogonal to the plane of the acyls with H_a–C(43)–C(42)–O(42) and H_a–C(43)–C(44)–O(44) torsion angles of −71.3 and −76.6°, respectively. Equatorial H_b is nearly in the plane of the acyls with H_b–(C43)–C(42)–O(42) and H_b–C(43)–C(44)–O(44) torsion angles of −165.4 and −179.4°, respectively. H_b is also at a 2.40 Å nonbonding contact from the nitrosyl nitrogen.

Discussion

1. Synthesis of μ-Malonyl Complexes. The reaction of a transition-metal enolate and a metal carbonyl electrophile, described herein, constitutes the first synthetic route into complexes of the parent μ-malonyl ligand. Thus, reaction of $[(\eta^5\text{-}C_5Me_5)(NO)(PPh_3)Re(COCH_2)]^-Li^+$ (**8**) with $(CO)_5M(OSO_2CF_3)$ [M = Re, Mn], $(CO)_5ReBr$, and $[(CO)_5Re(PMe_3)]^+OSO_2CF_3^-$ leads to three subclasses of μ-malonyl complexes: the neutral η^1,η^2-malonyls, **10-Re** and **10-Mn**; the anionic η^2,η^2-malonyl **17**; and the neutral η^2,η^2-malonyl **19**.

The reaction of enolate **8** and $(CO)_5Re(OSO_2CF_3)$ to give **10-Re** proceeds through an intermediate species that is observable by low-temperature ^1H, ^{31}P, and ^{13}C NMR spectroscopy. Both the spectroscopic evidence and trapping with PMe_3 (to give **19**) are consistent with a μ-malonyl structure (**16**) for this intermediate species (Scheme VIII).

A mechanism involving initial carbon–carbon bond formation between the metallaenolate and a carbonyl ligand of $(CO)_5Re(OSO_2CF_3)$ is also supported by the formation of an anionic malonyl (**17**) upon reaction of **8** and $(CO)_5ReBr$. The formation of **17** is consistent with Lukehart's prior observation[34] that MeLi and $(CO)_5ReBr$ give the anionic acyl **20** but is in marked contrast to a report[35] that the iron enolate $[(\eta^5\text{-}C_5H_5)(CO)(PPh_3)Fe(COCH_2)]^-Li^+$ (**6**) and $(CO)_5MBr$ (M = Mn, Re) give the unstable μ-ketene complex $(\eta^5\text{-}C_5H_5)(CO)(PPh_3)Fe[\mu\text{-}(COCH_2)\text{-}C^1{:}C^2]M(CO)_4$ (**21**, M = Re, Mn).

Table V. Selected Bond Distances and Angles for **19**

(a) Bond Distances (Å)

A–B	distance	A–B	distance
Re(1)–P(1)	2.386 (3)	St–Ot(3)	1.439 (10)
Re(1)–C(1)	2.349 (12)	St–Ct	1.776 (20)
Re(1)–C(2)	2.294 (13)	C(1)–C(2)	1.424 (17)
Re(1)–C(3)	2.303 (12)	N(41)–O(41)	1.200 (12)
Re(1)–C(4)	2.332 (12)	C(42)–O(42)	1.228 (12)
Re(1)–C(5)	2.374 (14)	C(42)–C(43)	1.563 (16)
Re(1)–N(41)	1.760 (9)	C(43)–H_a	0.935 (98)
Re(1)–C(42)	2.069 (9)	C(43)–H_b	0.939 (148)
Re(2)–P(2)	2.453 (5)	C(43)–C(44)	1.516 (16)
Re(2)–C(44)	2.194 (11)	C(44)–O(44)	1.254 (13)
Re(2)–C(45)	1.996 (13)	C(45)–O(45)	1.122 (16)
Re(2)–C(46)	2.002 (13)	C(46)–O(46)	1.121 (17)
Re(2)–C(47)	1.988 (15)	C(47)–O(47)	1.117 (19)
Re(2)–C(48)	1.963 (20)	C(48)–O(48)	1.120 (25)
P(1)–C(16)	1.844 (7)	Ct–Ft(1)	1.275 (24)
St–Ot(1)	1.432 (10)	Ct–Ft(2)	1.294 (25)
St–Ot(2)	1.431 (10)	Ct–Ft(3)	1.333 (30)

(b) Bond Angles (deg)

A–B–C	angle	A–B–C	angle
P(1)–Re(1)–N(41)	91.4 (3)	Ot(2)–St–Ct	103.7 (8)
P(1)–Re(1)–C(42)	86.6 (3)	Ot(3)–St–Ct	101.4 (9)
N(41)–Re(1)–C(42)	97.2 (4)	Re(1)–N(41)–O(41)	172.3 (9)
P(2)–Re(2)–C(44)	84.3 (3)	Re(1)–C(42)–O(42)	124.9 (8)
P(2)–Re(2)–C(45)	89.3 (5)	Re(1)–C(42)–C(43)	120.5 (7)
C(44)–Re(2)–C(45)	86.3 (5)	O(42)–C(42)–C(43)	114.6 (8)
P(2)–Re(2)–C(46)	88.2 (5)	C(42)–C(43)–C(44)	116.5 (9)
C(44)–Re(2)–C(46)	91.1 (5)	Re(2)–C(44)–C(43)	123.6 (7)
P(2)–Re(2)–C(47)	173.8 (4)	Re(2)–C(44)–O(44)	119.9 (8)
C(44)–Re(2)–C(47)	89.5 (5)	C(43)–C(44)–O(44)	116.4 (9)
C(45)–Re(2)–C(47)	89.6 (6)	Re(2)–C(45)–O(45)	179.7 (12)
C(46)–Re(2)–C(47)	92.7 (6)	Re(2)–C(46)–O(46)	178.5 (15)
P(2)–Re(2)–C(48)	95.2 (7)	Re(2)–C(47)–O(47)	177.2 (14)
C(44)–Re(2)–C(48)	176.8 (6)	Re(2)–C(48)–O(48)	179.4 (21)
C(45)–Re(2)–C(48)	90.6 (7)	St–Ct–Ft(1)	112.6 (15)
C(46)–Re(2)–C(48)	92.0 (7)	St–Ct–Ft(2)	113.1 (15)
C(47)–Re(2)–C(48)	91.0 (8)	Ft(1)–Ct–Ft(2)	112.2 (18)
Ot(1)–St–Ot(2)	114.6 (7)	St–Ct–Ft(3)	110.8 (15)
Ot(1)–St–Ot(3)	115.4 (6)	Ft(1)–Ct–Ft(3)	102.5 (19)
Ot(2)–St–Ot(3)	114.2 (6)	Ft(1)–Ct–Ft(3)	104.8 (18)
Ot(1)–St–Ct	105.2 (9)		

(34) Darst, K. P.; Lukehart, C. M. *J. Organomet. Chem.* **1979**, *171*, 65. See also: Drew, D.; Darensbourg, M. Y.; Darensbourg, D. J. *J. Organomet. Chem.* **1975**, *85*, 73. Parker, D. W.; Marsi, M.; Gladysz, J. A. *J. Organomet. Chem.* **1980**, *194*, C1.

(35) Geoffroy, G. L.; Bassner, S. L. *Adv. Organomet. Chem.* **1988**, *28*, 1.

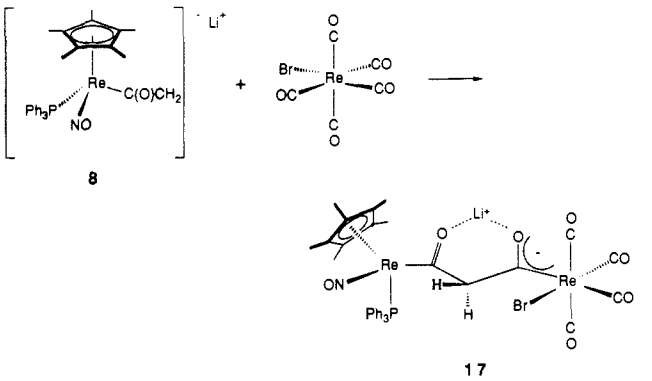

Chart IV

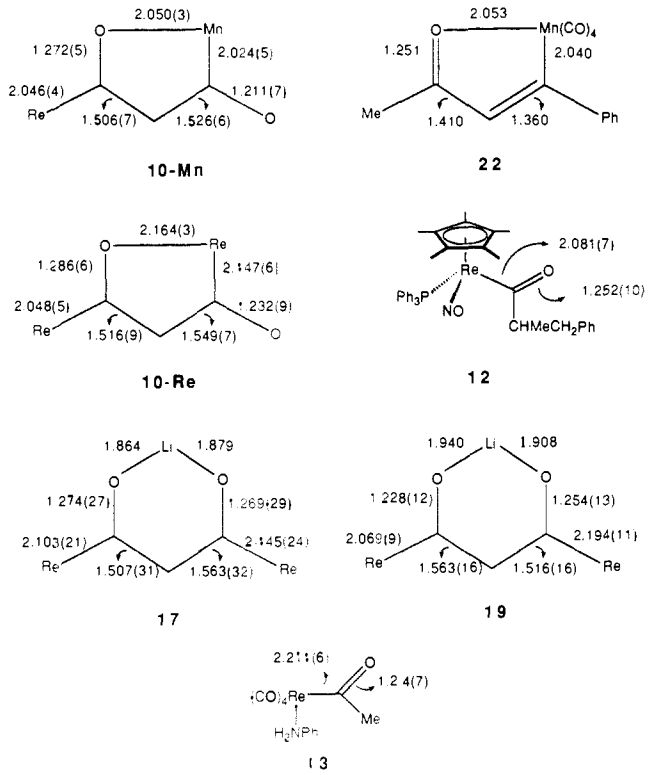

Chart V

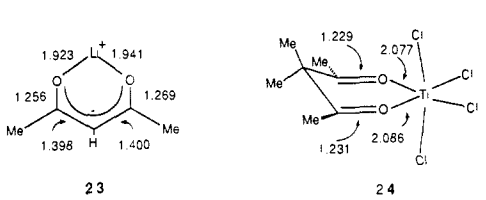

2. **Spectroscopic Characterization.** The key spectroscopic and structural properties for the μ-malonyl complexes **10**, **17**, and **19** are summarized in Table I and Chart IV. The ^{13}C NMR and X-ray data are consistent with carbenoid character at the metal–carbon bonds of the malonyl ligand (e.g. **10-M** ↔ **10-M-A** ↔ **10-M-B** and **19** ↔ **19-A**; Scheme X).

Isotopic labeling studies support assignment of the η^2-carbonyl stretch in the IR spectrum of **10-Re** to bands at 1394 and 1374 cm^{-1}. In the IR spectrum of mononuclear acyl **9** a carbonyl stretch is observed at 1555 cm^{-1}; thus, coordination of the acyl oxygen to $Re(CO)_4R$ results in a >140-cm^{-1} shift to lower wavenumber. The corresponding carbonyl stretch for **17** and **19** is observed at 1482 and 1500 cm^{-1}, respectively. The $Re(CO)_4R$ group thus serves as a stronger Lewis acid toward the acyl oxygen in **10-Re** than is the lithium ion in **17** or **19**. The acyl group bonded directly to the rhenium tetracarbonyl center in **19-Re**, **17**, and **19** exhibits IR bands at 1615, 1560, and 1570 cm^{-1}, respectively. For comparison, the IR spectra of $(CO)_5Re(COCH_3)$ and $[cis\text{-}(CO)_4(Br)Re(COCH_3)]^-Li^+$ exhibit bands at 1622 and 1565 cm^{-1}, respectively.[34,36]

In the $^{13}C\{^1H\}$ NMR spectra, the carbonyl carbons of the malonyl ligand in **10-Re** are observed at somewhat lower field than expected for a typical acyl carbonyl carbon: 298 ($C^1{=}O^1$) and 276 ($C^3{=}O$) ppm. The ^{13}C NMR chemical shift of the acyl carbon (C^1) bonded to the chiral rhenium center in **17** (270.8 ppm) and **19** (262.2 ppm) is very similar to that observed for **9**[20] (264.5 ppm). However, the acyl carbon bonded to the $Re(CO)_4$ center in **17** (270.7 ppm) and **19** (261.6 ppm) is significantly downfield from that observed for $(CO)_5Re(COCH_3)$ (244.7 ppm).[36] This increase in carbenoid character is attributed to the anionic charge in **17** and the presence of the PMe_3 donor ligand in **19**.

3. **Solid-State Structural Characterization.** A number of structural features of **10-Mn**, **10-Re**, **17**, and **19** deserve mention (Chart IV). The Re–C^1 bond distances in **10-Mn** and **10-Re** are nearly identical, 2.046 and 2.048 Å, respectively, indicative of a nearly identical degree of carbene character. The $Re(CO)_4R$ and $Mn(CO)_4R$ groups therefore serve as Lewis acids of comparable strength when coordinated to the acyl oxygen atoms of **10-Re** and **10-Mn**. The rhenium–carbon bond in **10-Re** is 0.37 Å shorter than the related bond distance in mononuclear complex **12**. Unexpectedly, the manganese–oxygen bond distance in **10-Mn** is nearly identical (2.053 Å) with that in the mononuclear manganacycle **22**,[23] despite a significantly longer carbon–oxygen distance in the chelate ring of **10-Mn** (1.272 (5) vs 1.251 Å). The manganese–carbon bond distance in **22** is 2.040 Å whereas the manganese–acyl carbon distance in **10-Mn** is somewhat shorter at 2.024 (5) Å. DeShong et al. previously discussed the structure of **22** in terms of partial Mn–C double bond character and suggested that **22** has, by some criteria, aromatic character.[37]

The unusual chemical shifts for the methylene hydrogens of **17** (δ 5.81 and 1.94) and **19** (δ 5.18 and 1.48) are readily explained from the solid-state structures of each complex. In both complexes the malonyl–lithium chelate ring exists in a boat conformation with one axial and one equatorial methylene hydrogen. The axial hydrogens are on the same side of the chelate ring as the PPh_3 ligand, with the hydrogen atom positioned in the shielding region of one of the phenyl rings on the phosphine ligand.[38] In the case of **19**, for which the hydrogens were located on a difference map and refined, the axial hydrogen is at a 2.78-Å nonbonded distance from the centroid of the phenyl ring. On the other hand, the equatorial hydrogen in both complexes is situated in the deshielding cone of both carbonyls of the malonyl ligand.

The structural data for **19** are of particular interest as they represent the first structural characterization of alkali metal chelation by a neutral malonyl compound. The malonyl oxygen–lithium distances are very similar to those observed in the malonate–lithium complex **23**, as shown in Chart V.[39] An adduct of titanium tetrachloride with 3,3-dimethyl-2,4-pentanedione (**24**) has also been structurally characterized, and the relevent bond distances are included in Chart V.[40] Unlike **19**, for which the six-membered chelate ring adopts a boat conformation, in **24** the chelate ring is in a nearly planar conformation with the carbon bearing the geminal methyl substituents slightly puckered (16.6°) out of the mean plane. A boat conformation in **24** would lead to an unfavorable 1,4-diaxial interaction between a methyl substituent and a chloride ligand on titanium. The carbon–oxygen bond distances are significantly shorter and the oxygen–metal distances significantly longer in **24** than those observed in **19**. The ionic radii of the lithium cation and titanium(4+) are similar[41]

(36) Darst, K. P.; Lukehart, C. M.; Warfield, L. T.; Zeile, J. V. *Inorg. Synth.* **1980**, *20*, 200.
(37) DeShong, P.; Slough, G. A.; Sidler, D. R.; Rybczynski, P. J.; Von Philipsborn, W.; Kunz, R. W.; Bursten, B. E.; Clayton, T. W., Jr. *Organometallics* **1989**, *8*, 1381.
(38) Haigh, C. W.; Mallion, R. B. *Org. Magn. Reson.* **1972**, *4*, 203.
(39) Schröder, F. A.; Weber, H. P. *Acta Crystallogr.* **1975**, *B31*, 1745.
(40) Maier, G.; Seipp, U.; Boese, R. *Tetrahedron Lett.* **1984**, *25*, 645.
(41) Pauling, L. *The Nature of the Chemical Bond*, 3rd ed.; Cornell University: Ithaca, NY, 1960; p 516.

Scheme VIII

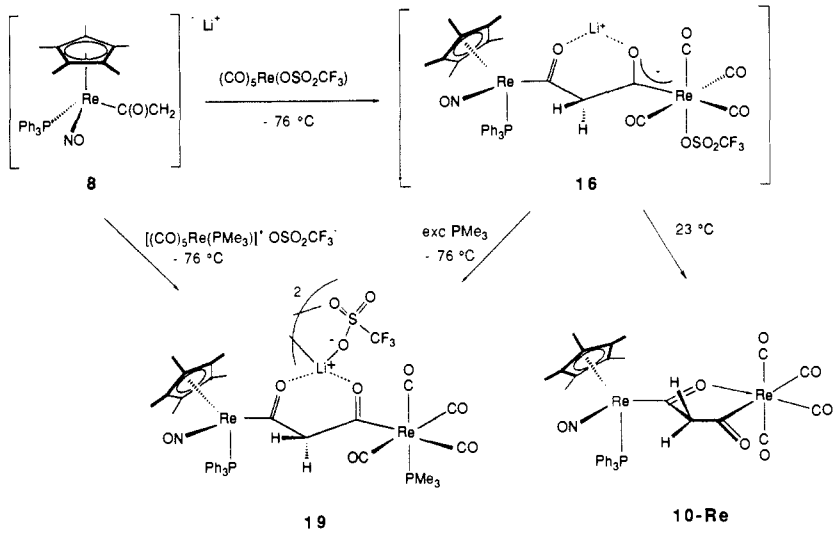

Scheme IX

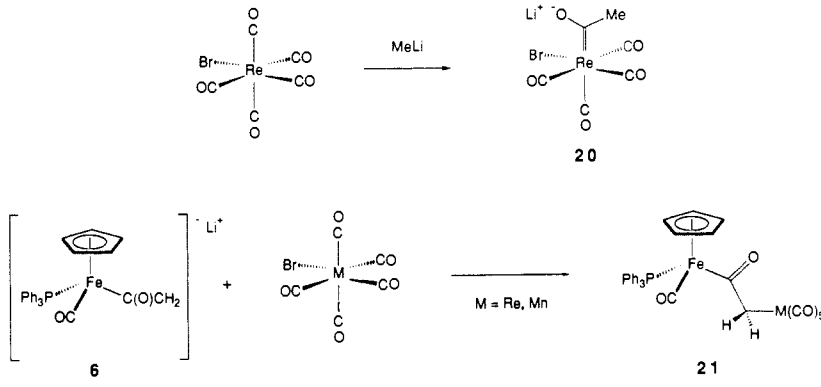

Scheme X

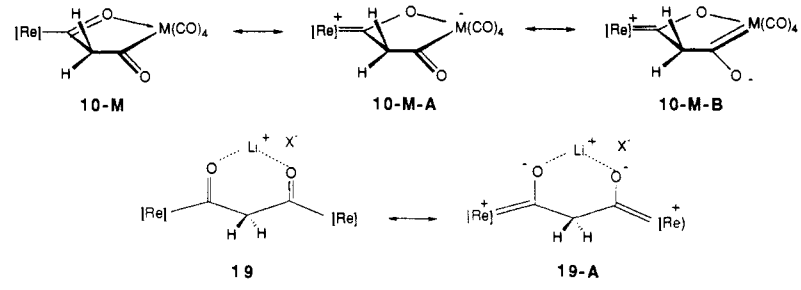

and we attribute the observed bond distance variations between **19** and **24** largely to the carbenoid character in the metal–carbon bonds of **19**.

4. Relationship of Differential $^2J_{CH}$ Coupling to Structure. Significant differential $^2J_{CH}$ coupling was observed between the ^{13}C-enriched carbonyl carbon and the methylene hydrogens of the malonyl ligand in **17-^{13}CO-A**, **17-^{13}CO-B**, **19-^{13}CO-A**, and **19-^{13}CO-B**. In contrast, **10-^{13}CO-Re** exhibited $^2J_{CH}$ couplings of similar magnitude for each of the methylene hydrogens. The solid-state structures of **17** and **19** indicate that the malonyl ligand is in a six-membered chelate ring that adopts a boat conformation. In each case, the equatorial hydrogen is in the deshielding region of both carbonyls and is therefore assigned to the downfield resonance in the ^{1}H NMR spectra (for **17**, δ 5.82; for **19**, δ 5.18). The axial hydrogens are in the shielding region of a phenyl substituent of the PPh_3 ligand, consistent with the unusual upfield shift in the ^{1}H NMR spectrum (to δ 1.93 for **17** and δ 1.48 for **19**). For both **17** and **19** the upfield methylene resonance has a geminal carbon–hydrogen coupling of $^2J_{CH} \approx 5$ Hz whereas the downfield resonance exhibits no geminal carbon–hydrogen coupling. In the case of **10-Re** the solid-state structure indicates that the malonyl ligand exists in a slightly puckered five-membered chelate ring. The pseudoaxial and pseudoequatorial hydrogens exhibit similar $^2J_{CH}$ couplings, 1.6 and 2.2 Hz, respectively.[42] The differential $^2J_{CH}$ coupling observed in **17** and **19** therefore appears to be diagnostic of a favored nonplanar malonyl ligand conformation. In **10-Re** both methylene hydrogens exhibited a similar H–C–C–O dihedral angle in the solid state, whereas for **17** and **19** the dihedral angle is much different for the axial and equitorial hydrogens. We anticipate, on the basis of the above analysis, that differential $^2J_{CH}$ coupling will also be observed in mononuclear acyls for which a favored nonplanar conformation exists. As a preliminary test of this hypothesis we prepared the mononuclear trimethylsilyl-substituted acyl **25**, with ^{13}C-enrichment at the carbonyl carbon. The steric bulk associated with the $-SiMe_3$ substituent and the favored 180° ON–Re–C_α–O torsion angle are expected to induce a conformational preference in which the $-SiMe_3$ group is located above the $ReC_\alpha(=O)C_\beta$ plane, away from

(42) The axial and equatorial hydrogen assignments in the ^{1}H NMR spectrum of **10-Re** are based on deuterium incorporation studies, NOE studies, and chemical shift arguments: see ref 5.

the PPh_3 ligand. Indeed, in the ^1H NMR spectrum of **25-^{13}CO** a significant differential $^2J_{CH}$ coupling is observed: δ 2.25 (dd, J = 11.5, 2.9 Hz, 1 H) and 1.16 (dd, J = 11.4, 6.1 Hz, 1 H). As anticipated, the corresponding methyl-substituted acyl complex **26-^{13}CO** exhibits $^2J_{CH}$ couplings of similar magnitude for each methylene hydrogen: δ 2.20 (m, $^2J_{CH}$ = 4.0 Hz, 1 H) and 1.98 (m, $^2J_{CH}$ = 3.4 Hz, 1 H).

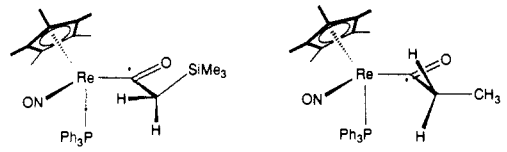

25-^{13}C O 26-^{13}C O

• ≡ ^{13}C • ≡ ^{13}C

Geminal carbon–hydrogen couplings have previously been employed for the conformational analysis of carbohydrates[43] and for determination of configuration in substituted alkenes.[44] On the basis of the limited data currently at hand it appears that geminal carbon–hydrogen couplings in carbonyl compounds will also find useful application in conformational analysis.[45]

Conclusion

The first stable complexes of the parent μ-malonyl ligand have been prepared from reaction of a mononuclear metallaenolate and metal carbonyl electrophile. Evidence was presented to support a mechanism involving attack of the enolate directly at a carbon monoxide ligand of the electrophile. When the metal carbonyl contains the triflate leaving group, $(CO)_5Re(OSO_2CF_3)$, a five-membered-ring oxametallacycle (**10-Re**, **10-Mn**) forms upon warming the reaction mixture to room temperature. With the less labile bromide leaving group, $(CO)_5ReBr$, an anionic μ-malonyl complex (**17**) is isolated, in which both malonyl oxygens are coordinated to the lithium counterion. In the case of the cationic metal carbonyl electrophile, $(CO)_5Re(PMe_3)^+$, a neutral malonyl complex (**19**) is isolated in which the malonyl oxygens coordinate to a lithium triflate salt. The formation of **17** is in surprising contrast to the reported formation of μ-ketene complex **21** upon reaction of the related iron enolate **6** and $(CO)_5ReBr$.[35]

X-ray crystallographic studies on each of the three subclasses of malonyl complex confirm the proposed structures and shed light on the unusual spectroscopic properties and bonding in these compounds. In each case a significant degree of carbene character is indicated for the metal–carbon bonds of the malonyl ligand. The solid-state structure determination of **19** is the first structural characterization of alkali metal chelation by a neutral malonyl compound. The six-membered chelate ring exists in a boat conformation and the lithium–oxygen bond distances are in the same range as that observed in malonate–lithium chelates. These relatively short oxygen–lithium distances in **17** and **19** are undoubtedly a consequence of the carbenoid character in the metal–acyl bonds of the malonyl ligand. Chelation of the lithium ion by the malonyl oxygens leads to a favored conformational preference for the malonyl ligand and a remarkably large chemical shift difference for the malonyl hydrogens in the ^1H NMR spectrum. The favored nonplanar conformation of the malonyl chelate ring also results in differential $^2J_{CH}$ coupling between the carbonyl carbons and the methylene hydrogens of the malonyl ligand. This differential coupling appears to provide a useful diagnostic test for distinguishing planar and nonplanar malonyl ligand conformations. To date no complexes of the parent nonchelating μ-malonyl ligand have been isolated, and it appears that chelation of the malonyl oxygens to an additional metal may prove to be a useful strategy for stabilization of μ-malonyl compounds.

Experimental Section

General. All manipulations, unless otherwise stated, were performed under purified nitrogen with schlenk techniques or in a Vacuum Atmospheres nitrogen box equipped with a Dri-Train MO 40-1 purifier. Infrared (IR) spectra were recorded on a Perkin-Elmer 1330 infrared spectrophotometer. Melting points were determined in sealed capillaries on an Electrothermal melting point apparatus and are reported uncorrected. Mass spectra were performed at the University of California, Riverside Mass Spec (UCRMS) facility. Elemental analyses were performed by Desert Analytics, Galbraith Laboratories, or Schwarzkopf. ^1H and ^{13}C and ^{31}P NMR spectra were recorded at ambient probe temperature unless otherwise stated on a GE QE 300 NMR spectrometer: ^1H, 300 MHz; ^{13}C, 74 MHz, ^{31}P, 121 MHz. ^1H NMR chemical shifts are reported relative to the residual protiated solvent resonance: $CDHCl_2$, δ 5.32; $CHCl_3$, δ 7.24; THF-d_7, δ 3.58. ^{13}C NMR chemical shifts are reported relative to the solvent resonance: $CDCl_3$, δ 77.0; CD_2Cl_2, δ 53.8; THF-d_8, δ 67.4. ^{31}P NMR chemical shifts are reported relative to external 85% H_3PO_4. Dried and degassed solvents were used throughout. Tetramethylethylenediamine (TMEDA) was vacuum distilled from sodium and stored over activated 4 Å molecular sieves. ^{13}CO gas, 99.4% ^{13}C and 13.3% ^{18}O enriched, was purchased from Isotec Inc., Ohio. $[(CO)_5Re(PMe_3)]^+O_3SCF_3^-$ was prepared from $(CO)_5Re(O_3SCF_3)$ and PMe_3. The complexes $(\eta^5\text{-}C_5Me_5)(NO)(PPh_3)Re(COCH_3)$ (**9**),[20] $(\eta^5\text{-}C_5Me_5)(NO)(PPh_3)Re(CH_3)$,[46] $[(\eta^5\text{-}C_5Me_5)(NO)(PPh_3)Re(CO)]^+BF_4^-$ (**11**),[46] $(CO)_5Re(OSO_2CF_3)$, and $(CO)_5Mn(OSO_2CF_3)$[47] were prepared from literature procedures.

Preparation of $(\eta^5\text{-}C_5Me_5)(NO)(PPh_3)Re[\mu\text{-}(COCH_2CO)\text{-}C^1{:}C^3,O^1]Mn(CO)_4$ (10-Mn). A round-bottomed flask equipped with a magnetic stir bar was charged with **9** (1.59 g, 2.42 mmol, 0.07 M) and 35 mL of THF. After the solution was cooled to −76 °C, a 1.6 M solution of *n*-BuLi in hexanes (0.98 mL, 2.45 mmol) was added via syringe, and the resulting deep red solution stirred at −76 °C for 0.5 h. This solution was then transfered via cannula to a stirred −76 °C THF (50 mL) solution of $(CO)_5Mn(OSO_2CF_3)$ (0.83 g, 2.42 mmol, 0.05 M). The resulting orange solution was stirred at −76 °C for 0.5 h, warmed to room temperature, and then passed through a short column of silica gel in the air. The column was washed with THF–hexanes (1:1 v/v) until the eluant was clear. The solvent was then removed by rotary evaporation, and the orange residue was dissolved in CH_2Cl_2. Hexanes was added, and the yellow precipitate (**10-Mn**) was collected by filtration (0.92 g, 1.08 mmol). A second crop of **10-Mn** was obtained from the mother liquor by recrystallization from THF–hexanes overnight in a −15 °C freezer, to give **10-Mn** as a yellow crystalline solid (60 mg, 0.07 mmol). The combined yield of **10-Mn** was 48%: mp 178–188 °C dec; $^{13}C\{^1H\}$ NMR (CD_2Cl_2) δ 283.2 (d, J = 10.0 Hz, Re*C*OCH$_2$), 282.3 (CH$_2$*C*OMn), 219.4 (Mn*C*O), 216.1 (Mn*C*O), 212.6 (Mn*C*O), 211.8 (Mn*C*O), 134.2 (m, *C*$_6$H$_5$) 131.1 (*C*$_6$H$_5$), 129.0 (*C*$_6$H$_5$), 128.9 (*C*$_6$H$_5$), 104.2 (*C*$_5$Me$_5$), 90.3 (CO*C*H$_2$CO), 10.4 (C$_5$*Me*$_5$); MS (FAB), *m/e* 851 (M^+), matched calcd isotopic distribution pattern for $C_{35}H_{32}NO_7PMnRe$. Anal. Calcd for $C_{35}H_{32}NO_7PMnRe$: C, 49.41; H, 3.79; N, 1.65. Found: C, 49.57; H, 4.01; N, 1.52.

Preparation of $(\eta^5\text{-}C_5Me_5)(NO)(PPh_3)Re[\mu\text{-}(COCH_2CO)\text{-}C^1{:}C^3,O^1]Re(CO)_4$ (10-Re). A 50-mL round-bottomed flask equipped with a magnetic stir bar was charged with **9** (1.12 g, 1.71 mmol, 0.04 M) and 40 mL of THF. After the solution was cooled to −76 °C, a 1.6 M solution of *n*-BuLi in hexanes (1.07 mL, 1.71 mmol) was added via syringe, and the resulting deep red solution was stirred at −76 °C for 0.5 h. This solution was then added via cannula to a stirred −76 °C THF (50 mL) solution of $(CO)_5Re(OSO_2CF_3)$ (0.81 g, 1.71 mmol, 0.03 M) in a 100-mL round-bottomed flask. The resulting orange solution was stirred at −76 °C for 1 h, warmed to room temperature, concentrated under vacuum to 40 mL, and charged with 15 mL of hexanes. A yellow precipitate (**10-Re**) was collected by filtration in the air and washed with three 30-mL portions of THF/hexanes (1:1 v/v). The solvent from the mother liquor was removed by rotary evaporation, and the residue was dissolved in CH_2Cl_2 and filtered through a plug of silica gel. The filtrate was concentrated, hexanes added, and the yellow precipitate (**10-Re**) washed with small portions of benzene. The combined yield of **10-Re** was 71% (1.20 g, 1.22 mmol): mp 195–200 °C dec; ^{13}C NMR ($CDCl_3$) δ 289.8 (d, J = 7.4 Hz (PPh$_3$)Re*C*OCH$_2$), 275.6 (CH$_2$*C*ORe(CO)$_4$), 194.9 (Re*C*O), 191.6 (Re*C*O), 191.4 (Re*C*O), 190.9 (Re*C*O), 133.3 (br m, *C*$_6$H$_5$), 130.9 (*C*$_6$H$_5$), 128.8 (*C*$_6$H$_5$), 128.7 (*C*$_6$H$_5$), 103.6 (*C*$_5$Me$_5$), 95.7

(43) Schwarcz, J. A.; Perlin, A. S. *Can. J. Chem.* **1972**, *50*, 3667. Cyr, N.; Hamer, G. K.; Perlin, A. S. *Can. J. Chem.* **1978**, *56*, 297 and references therein.

(44) Weigert, F. J.; Roberts, J. D. *J. Phys. Chem.* **1969**, *73*, 449.

(45) In addition to further examples of structural correlations with $^2J_{CH}$ in metal acyl and organic carbonyl systems, development of a Karplus-like relationship will require analysis of the sign of the couplings.

(46) Patton, A. T.; Strouse, C. E.; Knobler, C. B.; Gladysz, J. A. *J. Am. Chem. Soc.* **1983**, *105*, 5804.

(47) Schmidt, S. P.; Basolo, F.; Jensen, C. M.; Trogler, W. C. *J. Am. Chem. Soc.* **1986**, *108*, 1894.

(t, J = 126.0 Hz, $COCH_2CO$), 9.9 (q, J = 127.7 Hz, C_5Me_5); MS (FAB), m/e 982 (M^+), matched calculated isotopic distribution pattern for $C_{35}H_{32}NO_7PRe_2$. Anal. Calcd for $C_{35}H_{32}NO_7PRe_2$: C, 42.81; H, 3.28; N, 1.43. Found: C, 42.71; H, 3.49; N, 1.39.

10-Re and 14-Re: ^1H NMR (THF-d_8) δ 1.73 (s, 15 H), 1.76 (s, 15 H), 2.47 (d, J = 20.5 Hz, 1 H), 3.01 (d, J = 20.5 Hz, 1 H), 6.28 (s, 1 H), 7.39, 7.84 (br, 15 H), 8.91 (s, 1 H); IR (THF) 3500–3100 (vw, vbr) 2075 (w, sh), 1966 (vs), 1928 (s), 1665 (m), 1631 (w) cm^{-1}; $^{13}C\{^1H\}$ NMR (THF-d_8) δ 10.0, 10.1, 96.3, 103.4, 104.5, 128.8, 128.9, 129.6, 130.0, 130.4, 131.0, 131.8, 133.2, 134.0 (br), 139.6, 189.7, 191.2, 192.8, 193.0, 193.6, 194.6, 196.4, 225.4, 265.3, and 269.8. The resonances for carbonyl carbons bound to the stereogenic rhenium atoms are too weak in intensity for a chemical shift to be unambiguously assigned. The $^{13}C\{^1H\}$ NMR resonances attributed to **14-Re** are very similar in chemical shift to those of the trimethylsilyl analogue, $(\eta^5\text{-}C_5Me_5)Re(NO)(PPh_3)(COCHCOSiMe_3)Re(CO)_4$,[20] which has resonances in CD_2Cl_2 solution at δ 272.6 (d, J_{PC} = 11.0 Hz), 223.6, 193.9, 193.87, 190.8, 189.3, 145.2, 134.1, 130.6, 128.5 (d, J_{PC} = 10.1 Hz), 103.2, 10.0, 0.9.

Preparation of $[(\eta^5\text{-}C_5Me_5)(NO)(PPh_3)Re(^{13}CO)]^+BF_4^-$ (11-^{13}CO). A 30-mL Parr bomb was charged with $(\eta^5\text{-}C_5Me_5)(NO)(PPh_3)Re(CH_3)$ (1.25 g, 2.0 mmol) in the glovebox, capped with a rubber septum, and taken to a fume hood. CH_2Cl_2 (18 mL, 0.11 M) was added via syringe, and the bomb was shaken and then cooled to −76 °C. $HBF_4{\cdot}OEt_2$ (120 mL, 1.4 mmol) was added via syringe, the bomb shaken once, and the septum replaced with the pressure gauge assembly. The bomb was then pressurized with 250 psi of ^{13}CO gas, shaken, allowed to warm to room temperature, and then warmed to 75 °C for one minute. The bomb was vented in the fume hood, the solution transferred to a round bottomed flask, and the solvent removed by rotary evaporation. The dark brown residue was washed with ether, dissolved in methylene chloride, filtered, and concentrated by rotary evaporation. Ether was layered onto the solution, which was then placed in a −15 °C freezer for 2 days. The resulting brown solid was washed with 4 mL of THF to give **11-^{13}CO** (445 mg, 31%) as a yellow solid: IR (CH_2Cl_2) 1960 (s, 1956 calcd), 1914 [w, $\nu(^{13}C^{18}O)$ satalite], 1743 (vs) cm^{-1}.

Preparation of $(\eta^5\text{-}C_5Me_5)(NO)(PPh_3)Re(^{13}COCH_3)$ (9-^{13}CO). The two-step literature procedure for preparation of the unlabeled complex **9** from **11-^{13}CO** was employed. **9-^{13}CO**: IR (CH_2Cl_2) 1631 (vs), 1510 (m, 1511 calcd); ^1H NMR ($CDCl_3$) δ 7.35 (br s, 15 H), 1.80 (d, $^2J_{CH}$ = 5.6 Hz, 3 H), 1.69 (s, 15 H).

Preparation of $(\eta^5\text{-}C_5Me_5)(NO)(PPh_3)Re[\mu\text{-}(^{13}COCH_2CO)\text{-}C^1{:}C^3,O^1]Re(CO)_4$ (10-^{13}CO-Re). A procedure analogous to that for preparation of **10-Re** was employed, using the labeled precursor **9-^{13}CO**. **10-^{13}CO-Re**: mp 195–200 °C dec; IR (CH_2Cl_2) 2080 (s), 1972 (vs), 1925 (vs), 1665 (s), 1617 (m), 1480 (w), 1434 (w), 1418 (w), 1390 (w), 1365 (m), 1336 (m) cm^{-1}; ^1H NMR ($CDCl_3$) δ 7.43, 7.30 (br s, 15 H), 3.13 (dd, $^2J_{HH}$ = 20.6 Hz, $^2J_{CH}$ = 1.6 Hz, 1 H), 2.49 (dd, $^2J_{HH}$ = 20.6 Hz, $^2J_{CH}$ = 2.2 Hz, 1 H), 1.75 (s, 15 H).

Preparation of $\{(\eta^5\text{-}C_5Me_5)(NO)(PPh_3)Re[\mu\text{-}(COCH_2CO)\text{-}C^1{:}C^3]Re(CO)_4(Br)\}^-Li^+$ (17). A round-bottomed flask equipped with a magnetic stir bar was charged with **9** (0.80 g, 1.22 mmol, 0.03 M) and 40 mL of THF. After the solution was cooled to −76 °C, a 1.6 M solution of n-BuLi in hexanes (0.78 mL, 1.25 mmol) was added via syringe, and the resulting deep red solution was stirred at −76 °C for 15 min. This solution was then transfered via cannula to a stirred −76 °C THF (100 mL) solution of $(CO)_5ReBr$ (0.50 g, 1.23 mmol, 0.01 M). The resulting orange solution was stirred at −76 °C for 15 min, warmed to room temperature, and concentrated under vacuum to ca. 10–15 mL. Twice the volume of hexanes was added via cannula, and **17**·2THF was then isolated as a yellow solid by filtration. ^1H NMR spectral analysis (CD_2Cl_2, TMEDA) of the yellow solid indicated the presence of 2 equiv of THF (79% yield). The THF was removed by twice precipitating a CH_2Cl_2 suspension of **15**·2THF with hexanes and then isolating the yellow solid (**17**) by filtration: mp 185–190 °C dec: IR (KBr) 2085 (w), 1976 (vs), 1914 (s), 1649 (m), 1518 (m), 1480 (w), 1433 (w) cm^{-1}; ^1H NMR (THF-d_8) δ 7.41 (br s, 15 H), 5.90 (d, J = 15.6 Hz, 1 H), 2.29 (d, J = 15.6 Hz, 1 H), 1.72 (s, 15 H). Anal. Calcd for $C_{35}H_{32}NO_7PBrRe_2Li$: C, 39.33; H, 3.02; N, 1.31; Br, 7.48. Found: C, 39.08; H, 3.18; N, 1.46; Br, 7.17. Complex **17** was further characterized in solution by adding, via syringe, 2 equiv of TMEDA to the appropriate suspension of **17**: ^{13}C NMR (CD_2Cl_2, TMEDA, 14 °C) δ 270.8 (d, J = 9.5 Hz, $(PPh_3)ReCOCH_2$), 270.7 ($CH_2COReBr$), 190.6 (ReCO), 190.2 (ReCO), 189.5 (ReCO), 189.4 (ReCO), 133.9 (br s, C_6H_5), 130.6 (C_6H_5), 128.6 (C_6H_5), 128.4 (C_6H_5), 102.8 (C_5Me_5), 97.0 (dd, J = 138.1, 120.8 Hz, $COCH_2CO$), 54.5 (tm, J = 134.0 Hz, TMEDA), 45.8 (qm, J = 133.4 Hz, TMEDA), 9.9 (q, J = 127.9 Hz, C_5Me_5).

Preparation of $\{(\eta^5\text{-}C_5Me_5)(NO)(PPh_3)Re[\mu\text{-}(^{13}COCH_2CO)\text{-}C^1{:}C^3]Re(CO)_4(Br)\}^-Li^+$ (17-^{13}CO-A). A procedure analogous to that for the preparation of unlabeled **17** was employed, using the labeled precursor **9-^{13}CO**. **17-^{13}CO-A**: mp 180–192 °C dec: IR (CH_2Cl_2, TMEDA) 2085 (m), 1985 (vs), 1910 (s), 1649 (m), 1561 (m), 1467 (m), 1460 (m), 1435 (w) cm^{-1}; ^1H NMR (CH_2Cl_2, TMEDA, 14 °C) δ 7.40 (m, 15 H), 5.81 (d, $^2J_{HH}$ = 15.2 Hz, 1 H), 1.93 (dd, $^2J_{HH}$ = 15.2 Hz, $^2J_{CH}$ = 5.3 Hz, 1 H), 1.70 (s, 15 H); TMEDA resonances observed at δ 2.39 (br s, 4 H), 2.20 (br s, 12 H); $^{13}C\{^1H\}$ NMR (CD_2Cl_2, TMEDA, 14 °C) δ 270.8 (d, $^2J_{CP}$ = 9.5 Hz, most intense resonance), 270.8 (d, $^2J_{CC}$ = 9.2 Hz), 190.6, 190.2, 189.5, 189.4, 134.0 (m), 130.6, 128.6, 128.5, 102.8, 97.0 (d, $^1J_{CC}$ = 18.5 Hz), 57.4, 45.8, 9.9; ^{13}C NMR (CD_2Cl_2, TMEDA, 14 °C) δ 270.8 (dd, $^2J_{CP}$ = 9.6 Hz, $^2J_{CH}$ = 5.1 Hz).

Preparation of $(^{13}CO)_5ReBr$. A 30-mL Parr bomb equipped with a magnetic stir bar was charged with $(CO)_5ReBr$ (546 mg, 1.34 mmol, 0.11 M), 12 mL of $CHCl_3$, and 350 psi of ^{13}CO gas (6.7 mmol). The bomb was then heated to 70 °C for 13 h with stirring. After the mixture was cooled to 23 °C, 456 mg of white crystalline solid $(^{13}CO)_5ReBr$ was collected by filtration in the air. The solvent was removed from the filtrate by rotary evaporation, and the residue was sublimed (80 °C, 0.001 Torr) to give an additional 30 mg of $(^{13}CO)_5ReBr$: sublimation temperature 100–130 °C; IR (CH_2Cl_2) 2136 (w), 2120 (m), 2100 (w), 2075 (m), 2045 (s), 2020 (s, br), 1995 (s, br), 1970 (s, br), 1960 (s), 1900 (m) cm^{-1}; ^{13}C NMR ($CDCl_3$) δ 177.6, 176.3.

Preparation of $\{(\eta^5\text{-}C_5Me_5)(NO)(PPh_3)Re[\mu\text{-}(COCH_2{}^{13}CO)\text{-}C^1{:}C^3]Re(^{13}CO)_4(Br)\}^-Li^+$ (17-^{13}CO-B). An analogous procedure to that for the preparation of unlabeled **17** was followed, with employment of the labeled precursor $(^{13}CO)_5ReBr$. **17-^{13}CO-B**: mp 182–192 °C dec; IR (CH_2Cl_2, TMEDA) 2065 (vw), 2040 (vw), 1960 (s), 1940 (vs), 1900 (m), 1866 (m), 1649 (m), 1560 (vw), 1527 (w), 1480 (w), 1467 (m), 1460 (m), 1433 (m) cm^{-1}; ^1H NMR (CD_2Cl_2, TMEDA, 14 °C) δ 7.40 (m, 15 H), 5.81 (d, $^2J_{HH}$ = 15.2 Hz, 1 H), 1.93 (dd, $^2J_{HH}$ = 15.2, $^2J_{CH}$ = 4.8 Hz), 1.93 (d, $^2J_{HH}$ = 14.7 Hz, 1 H), 1.70 (s, 15 H); TMEDA resonances observed at δ 2.39 (br s, 4 H), 2.20 (br s, 12 H).

Preparation of $\{(\eta^5\text{-}C_5Me_5)(NO)(PPh_3)Re[\mu\text{-}(COCH_2CO)\text{-}C^1{:}C^3]Re(CO)_4(Br)\}^-MgBr^+$ (18). A round-bottomed flask equipped with a magnetic stir bar was charged with **17** (298 mg, 0.28 mmol, 0.02 mM), $MgBr_2{\cdot}OEt_2$ (74 mg, 0.29 mmol), and 15 mL of CH_2Cl_2. The mixture was then stirred at room temperature for 10 min and filtered, leaving behind a white solid. After the dark yellow solution was concentrated to 10 mL under vacuum, 10 mL of hexanes was added, and the mixture was concentrated under vacuum to 15 mL. Complex **18** was isolated as a bright yellow solid by filtration (187 mg, 0.16 mmol, 57%): mp 184–191 °C dec; $^{13}C\{^1H\}$ NMR (THF-d_8, 15 °C) δ 283.1 ($BrReCOCH_2$), 273.1 [d, J = 7.3 Hz, $(PPh_3)ReCOCH_2$], 189.7 (ReCO), 189.6 (ReCO), 189.5 (ReCO), 188.7 (ReCO), 134.6 (m, C_6H_5), 132.7 (m, C_6H_5), 130.8 (m, C_6H_5), 129.0 (m, C_6H_5), 103.3 (C_5Me_5), 97.0 (CH_2), 9.5 (C_5Me_5). Anal. Calcd for $C_{35}H_{32}NO_7PRe_2Br_2Mg$: C, 36.05; H, 2.77; N, 1.20. Found: C, 36.11; H, 2.96; N, 1.17. Molecular weight by osmometry in methylene chloride 1233, calcd 1186.

Decomposition of $\{(\eta^5\text{-}C_5Me_5)(NO)(PPh_3)Re[\mu\text{-}(COCH_2CO)\text{-}C^1{:}C^3]Re(CO)_4(Br)\}^-Li^+$ (17). A 5-mm NMR tube was charged with **17** (23.8 mg, 0.0223 mmol, 67.5 mM), 12-crown-4 (2.7 equiv by NMR spectroscopy, 0.183 M), 1,4-bis(trimethylsilyl)benzene as an internal standard, and methylene-d_2 chloride (0.33 mL). The tube was then flame sealed under vacuum, and the decomposition of **17** was monitored by ^1H NMR spectroscopy over the next 119 h. The final product distribution was the following: **10-Re**, 52.8 mM (77%); **9**, 11.8 mM (18%); **11**, 6.1 mM (9%).

Preparation of $\{(\eta^5\text{-}C_5Me_5)(NO)(PPh_3)Re[\mu\text{-}(COCH_2CO)\text{-}C^1{:}C^3]Re(CO)_4(PMe_3)\}\cdot Li^+OSO_2CF_3^-$ (19). A round-bottomed flask equipped with a magnetic stir bar was charged with **9** (200 mg, 0.305 mmol, 0.05 M) and 6 mL of THF and then cooled to −76 °C. A 1.6 M solution of n-BuLi in hexanes (0.20 mL, 0.32 mmol) was added via syringe, and the resulting deep red solution was stirred at −76 °C for 15 min. This solution was then transfered via cannula to a stirred −76 °C THF (5 mL) solution of $(CO)_5Re(OSO_2CF_3)$ (148 mg, 0.312 mmol, 0.06 M). After the resulting solution was stirred at −76 °C for 15 min, PMe_3 (1.4 mL, 13.5 mmol) was added by vacuum transfer. The solution was then stirred at −76 °C for 15 min and then at −29 °C for 1 h. Next the solution was warmed to room temperature, after which the volatiles were removed under vacuum. ^1H NMR spectral analysis ($CDCl_3$) of the crude orange solid indicated an 81% yield of **19**. The crude product was dissolved in CH_2Cl_2 (ca. 20–30 mL) and hexanes (ca. 10–15 mL) was added via cannula. The cloudy solution was filtered and the solvent removed under vacuum. Recrystallization from methylene dichloride/diethyl ether gave pure **19** (168 mg, 0.138 mmol, 45%) as an orange microcrystalline solid: mp 181–184 °C dec; ^{13}C NMR ($CDCl_3$, 14 °C) δ 262.2 (m, $ReCOCH_2$), 261.6 (m, $ReCOCH_2$), 189.1 (d, J = 10.4 Hz, cis-$(PMe_3)ReCO$), 188.7 (d, J = 4.6 Hz, cis-$(PMe_3)ReCO$), 188.0 (d, J = 9.6 Hz, cis-$(PMe_3)ReCO$), 188.0 (d, J = 41.0 Hz, $trans$-$(PMe_3)ReCO$), 133.8 (br m, C_6H_5), 130.0 (C_6H_5), 128.3 (C_6H_5), 128.2 (C_6H_5), 120.2 (three lines of a quartet observed, J = 318.8 Hz, CF_3), 103.0 (C_5Me_5), 98.4 (dd, J = 134.8, 123.8 Hz, $COCH_2CO$), 17.9 (qd, J = 132.7, 34.1 Hz, PMe_3), 9.9 (q, J = 127.9

Hz, C_5Me_5). Anal. Calcd for $C_{38}H_{41}NO_7P_2Re_2 \cdot LiO_3SCF_3$: C, 38.58; H, 3.40; N, 1.15. Found: C, 38.59; H, 3.39; N, 1.13.

Preparation of 19 from $[(CO)_5Re(PMe_3)]^+OSO_2CF_3^-$. A round-bottomed flask equipped with a magnetic stir bar was charged with **9** (75 mg, 0.114 mmol, 0.01 mM) and 8 mL of THF and then cooled to −76 °C. A 1.6 M solution of *n*-BuLi in hexanes (73 μL, 0.117 mmol) was added via syringe, and the resulting deep red solution was stirred at −76 °C for 0.5 h. This solution was then added via cannula to a stirred −43 °C THF (35 μL) solution of $[(CO)_5Re(PMe_3)]^+OSO_2CF_3^-$ (63 mg, 0.114 mmol, 3.3 mM) in a round-bottomed flask. The resulting dark orange solution was slowly warmed to room temperature and concentrated to ca. 10 mL under vacuum. After addition of ca. 20 mL of hexanes, a brown-orange solid (90 mg) was isolated by filtration. ^1H NMR analysis ($CDCl_3$, 1,4-$(TMS)_2C_6H_4$ as internal standard) indicated **19** was formed in 42% yield.

Reaction of 19 with D_2O. A 5-mm NMR tube was charged with **19** (8.5 mg, 0.007 mmol, 12 mM) and chloroform-*d* (0.6 mL) and sealed with a septum under a stream of nitrogen gas. Deuterium oxide (25 μL, 1.3 mmol) was added by syringe, and the resulting heterogeneous solution was vigorously shaken. A ^1H NMR spectrum of the sample indicated complete conversion of **19** to a new species with NMR resonances at δ 7.4 (br s, 15 H), 3.96 (d, J = 15.5 Hz, 1 H), 2.72 (d, J = 15.5 Hz, 1 H), 1.70 (s, 15 H), 1.60 (d, J = 9.3 Hz, 9 H). There was no evidence in the NMR spectrum for formation of an enol tautomer. The new complex decomposed over the course of hours to give a 70% yield of **11** as the major identifiable product by ^1H NMR spectroscopy. Preparative scale extraction of chloroform solutions of **19** with H_2O was unsuccessful and resulted in isolation of **19** along with variable amounts of **11** and **9**.

Preparation of $\{(\eta^5\text{-}C_5Me_5)(NO)(PPh_3)Re[\mu\text{-}(^{13}COCH_2CO)\text{-}C^1{:}C^3]\text{-}Re(CO)_4(PMe_3)\}\cdot Li^+OSO_2CF_3^-$ (19-^{13}CO-A). This complex was synthesized following a procedure analogous to that for preparation of unlabeled **19**, using $(^{13}CO)_5Re(OSO_2CF_3)$. The labeled triflate $(^{13}CO)_5Re(OSO_2CF_3)$ was prepared from metathesis of $(^{13}CO)_5ReBr$ with $Ag(OSO_2CF_3)$. **19-^{13}CO-A**: IR ($CHCl_3$) 2063 (w), 2051 (w), 1963 (s), 1941 (vs), 1918 (s), 1645 (m), 1539 (w), 1485 (vw), 1460 (vw), 1435 (w), 1421 (vw) cm^{-1}; ^1H NMR ($CDCl_3$) δ 7.42 (m, 15 H), 5.15 (d, $^2J_{HH}$ = 14.9 Hz, 1 H), 1.72 (s, 15 H), 1.60 (d, J = 9.4 Hz, 9 H), 1.48 (br d, $^2J_{HH}$ = 15.4 Hz, $\nu_{1/2}$ > 5 Hz).

Preparation of $(\eta^5\text{-}C_5Me_5)(NO)(PPh_3)Re(COCH_2SiMe_3)$ (25). A round-bottomed flask equipped with a magnetic stir bar was charged with **9** (163 mg, 0.248 mmol, 31 mM) and THF (8 mL) and then cooled to −76 °C. A 1.6 M solution of *n*-BuLi in hexanes (0.18 mL, 0.288 mmol) was added via syringe, and the resulting deep red solution was stirred for 0.5 h at −76 °C. Chlorotrimethylsilane (0.4 mL, 5.1 mmol) was added by vacuum transfer, and the resulting light red solution was stirred for 0.5 h at −76 °C and then allowed to warm to room temperature. The volatiles were then removed under vacuum, and the residue was taken up in CH_2Cl_2 and hexanes and then filtered. The solvent was removed from the filtrate under vacuum, and the residue was dissolved in a minimum of toluene. Hexanes was added until a precipitate formed, the mixture was filtered, and the filtrate was then placed in a −15 °C freezer. **25** was isolated by filtration as orange crystals (88 mg, 0.121 mmol, 49%): mp 176–179 °C dec; ^1H NMR (chloroform-*d*) δ 7.40 (m, 15 H), 2.26 (d, J = 11.5 Hz, 1 H), 1.70 (s, 15 H), 1.16 (d, J = 11.5 Hz, 1 H), −0.08 (s, 9 H); $^{13}C\{^1H\}$ NMR (chloroform-*d*) δ 262.2 (d, J = 6.4 Hz, ReCO), 134.0 (C_6H_5), 129.9 (C_6H_5), 128.1 (C_6H_5), 128.0 (C_6H_5), 102.3 (C_5Me_5), 9.8 (C_5Me_5), −0.6 ($SiMe_3$); IR (methylene chloride) 1627 (s), 1505 (m) cm^{-1}.

Preparation of $(\eta^5\text{-}C_5Me_5)(NO)(PPh_3)Re(^{13}COCH_2SiMe_3)$ (25-^{13}C-O). This complex was prepared following a procedure analogous to that used for unlabeled **25**, using **9-^{13}CO** (16.9 mg). The crude product was dissolved in methylene chloride and hexanes and then filtered. ^1H NMR (chloroform-*d*) analysis indicated a 31:69 mixture of **11-^{13}CO** and **25-^{13}CO**. **25-^{13}CO**: δ 7.40 (m, PPh_3), 2.25 (dd, J = 11.5, 2.9 Hz, 1 H), 1.70 (d, J = 0.3 Hz, 15 H), 1.16 (dd, J = 11.4, 6.1 Hz, 1 H), 0.08 (s, 9 H).

Preparation of $(\eta^5\text{-}C_5Me_5)(NO)(PPh_3)Re(^{13}COCH_2CH_3)$ (26-^{13}CO). This complex was prepared as in the literature procedure for unlabeled **26**,[20] using **9-^{13}CO** (11.5 mg). **27-^{13}CO** was isolated as a yellow oily solid by silica gel chromotography) 5% acetone in CH_2Cl32): ^1H NMR (chloroform-*d*) δ 7.40 (m, 15 H), 2.20 (m, $^2J_{CH}$ = 4.0 Hz, 1 H), 1.98 (m, $^2J_{CH}$ = 3.4 Hz, 1 H), 1.71 (s, 15 H), 0.48 (td, $^3J_{HH}$ = 7.3 Hz, $^3J_{CH}$ = 4.6 Hz, 3 H).

X-ray Structure Determinations for 10-Re and 19. Crystallographic data are summarized in Table II. Specimens for both compounds, which were found satisfactory for diffraction studies, were mounted on glass fibers. Both photographic and diffraction data were used in the assignment of space groups (**10-Re**, $P1$; **19**, $C2/c$); the chemical reasonableness of the results supports these choices.

Data were collected with a Nicolet R3m/μ diffractometer at the University of Delaware. The structures were solved by Patterson syntheses and completed by subsequent difference Fourier synthesis. All non-hydrogen atoms were refined with anisotropic thermal parameters, all hydrogen atoms idealized, except for the bridging methylene hydrogen atoms of the malonyl ligand in **19**, which were located on a difference map and refined. The phenyl rings were constrained to rigid planar hexagons. All computations used SHELXTL (5.1) software which also served as the source for the scattering factors (G. Sheldrick, Nicolet XRD, Madison, WI). The supplementary material for **19** was deposited previously. For **10-Re**, tables of fractional coordinates, bond distances, bond angles, hydrogen atom coordinates, and thermal parameters are given as Supplementary Material.

X-ray Structure Determination for 17·TMEDA. A summary of crystallographic data is given in Table I. Crystals were grown by slow addition of dibutyl ether to a dichloroethane solution of **17**·TMEDA. Data were collected with a Nicolet R3m/V diffractometer at the University of California at San Diego. Since crystal decomposition was rapid, the data were collected at −100 °C. The intensities of three monitor reflections, measured after every 100 reflections, decayed by ca. 15% during 65 h of X-ray exposure; this was corrected by applying appropriate scaling factors. The cell parameters were obtained from 20 reflections in the range $15 < 2\theta < 30°$. The systematic absences ($0k0$, $k = 2n + 1$, $h0l$, $h + l = 2n + 1$) identified the space group as $P21/n$. The data were corrected for absorption (analytical), Lorentz, and polarization effects. The Re and P atoms were obtained from the automatic direct methods routine of the program SHELXTL plus. The positions of the remaining non-hydrogen atoms were determined from a difference Fourier map. The Re, Br, Cl, P, and oxygen atoms (except O(41) and O(44)) were refined anisotropically. Hydrogen atoms were then included in subsequent refinements in ideal positions. The inability to refine O(41), O(44), N(41), and Li atoms anisotropically suggested some evidence of positional disorder.

Positional and thermal parameters, interatomic distances and bond angles, and a cell packing diagram are given as supplementary material.

Acknowledgment. Partial support of the National Science Foundation (CHE-8721344) is gratefully acknowledged. The NMR spectrometer utilized was acquired via an NIH instrumentation grant (NIH-1S10RR02652-01) and the UCSD diffractometer was acquired via an NSF instrumentation grant (CHE-8904832).

Supplementary Material Available: Tables of atomic coordinates and isotropic thermal parameters, bond lengths and angles, anisotropic thermal parameters and displacement coefficients, and hydrogen atom coordinates for **17** and **10**-Re (11 pages); listing of observed and calculated structure factors (59 pages). Ordering information is given on any current masthead page.